



UNIVERSITY OF LEEDS

This is a repository copy of *Multiphysics Modeling and Simulation of the Effective Thermal Conductivity of Polymeric Composites*.

White Rose Research Online URL for this paper:

<https://eprints.whiterose.ac.uk/152877/>

Version: Accepted Version

Book Section:

Ocheme, SE and Antony, SJ orcid.org/0000-0003-1761-6306 (2019) Multiphysics Modeling and Simulation of the Effective Thermal Conductivity of Polymeric Composites. In: James, J, Pallathadka, PK and Thomas, S, (eds.) Polymers and Multicomponent Polymeric Systems: Thermal, Thermo-Mechanical and Dielectric Analysis. CRC Press , Boca Raton , pp. 119-152. ISBN 9781138598140

<https://doi.org/10.1201/9780429486609>

© 2020 by Taylor & Francis Group, LLC. This is an Accepted Manuscript of a book chapter published by CRC Press in Polymers and Multicomponent Polymeric Systems: Thermal, Thermo-Mechanical and Dielectric Analysis on December 10, 2019, available online: <http://www.routledge.com/9781138598140>.

Reuse

Items deposited in White Rose Research Online are protected by copyright, with all rights reserved unless indicated otherwise. They may be downloaded and/or printed for private study, or other acts as permitted by national copyright laws. The publisher or other rights holders may allow further reproduction and re-use of the full text version. This is indicated by the licence information on the White Rose Research Online record for the item.

Takedown

If you consider content in White Rose Research Online to be in breach of UK law, please notify us by emailing eprints@whiterose.ac.uk including the URL of the record and the reason for the withdrawal request.



eprints@whiterose.ac.uk
<https://eprints.whiterose.ac.uk/>

Chapter 28: Multiphysics modelling and simulation of the effective thermal conductivity of polymeric composites

S.E Ocheme & S.J Antony

School of Chemical and Process Engineering, University of Leeds, LS2 9JT, UK

The research rat of the future allows experimentation without the manipulation of the real (physical) world. This is the cutting edge of modelling technology (John Spencer)

Chapter Overview

The complex nature of heterogeneous material fillers either in a single or multi matrix composite structure provides a daunting challenge to scientists and engineering practitioners, in determining the effective thermal and electrical properties of the composite. A priority in modelling the thermal properties of these emerging materials that define the materials of the 4th industrial revolution is important to make them suitable for broad engineering applications. This class of problems are inherently Multiphysics; fortunately, we now have tools that couple diverse and complex phenomena to reduce dependency on building prototypes during the new material conception phase. This approach provides research engineers array of tools to build a digital twin of the “would be” particulate materials and calculate its thermal and electrical properties from fundamental principles. Modelling and simulation divided broadly into 2 class: empirical and fundamental. Empirical modelling is data-driven, supported by data analysis and statistics. Whereas, fundamental modelling uses the laws of evidence driven by set of conservation equations (for example Fourier Law, Maxwell Law etc.). As a starting point, empirical models assist the modeller organise and interpret data, providing useful quantitative relationships. Fundamental models provide applicable theory and new understanding, both qualitatively and quantitatively, facilitating further development and efficient management of knowledge. In this chapter, we will provide a Multiphysics approach for estimating the thermal and electrical properties of multi-filler and multi-matrix particulate composites with strong complement from experimental modelling.

1 Introduction

The increasing interest in low and high conductivity materials, serving as two extremes of heat retention and heat removal in the case of aerogel and graphene/carbon nanotubes requires characterisation, of these emerging and interesting new materials. The base materials – aerogel and graphene or carbon nanotubes- are embedded in a matrix or binders to form a single material called a composite with its own unique intrinsic property. The unique property is an effective one, considering the individual properties of the separate materials constituting the composite. The

effective properties, specifically the intrinsic effective thermal conductivity have been investigated by many investigations in the past [1–4]. A numerical approach investigating the thermal conductivity of polymeric composite was elucidated by Eian and Deissler [5]. The numerical techniques were extended by these authors to cover process systems for absorption and distillation columns packed bed applications [6–8]. The different forms and types of composite materials, such as long-fibre-reinforced, short-fibre-reinforced, laminates, and particulate, are used in applications in the aerospace, automobile, electronic and other industries. The application of composite material also covers a broad and extensive one as noted by [9]. These include but not limited to flying vehicles and all its associated parts, construction panels, jet stators, aircraft nose and cones, main helicopter rotors, racks and shields, etc.

Composite materials consisting of discrete solid constituents, find wide application in engineering, due to their superior mechanical and thermal properties, and lower cost, compared to the separate components. The complex, multiscale microstructures of these composites offer a veritable field for researching their behaviour at the micro and nano scales with respect to various transport processes, including heat transfer. The subject of heat transfer in composites is diverse. According to Furmanski [10], conduction is the most common and dominant form of heat transfer in such materials. The other form of heat transfer -convection and radiation modes- are of importance in special cases, such as when the composite has significant fluid-filled void content investigated by [11–14] and forced convection with an active cooling, or in open-cellular materials as observed by Kamiuto [15,16]. The determination of the effective thermal conductivity is thus the main goal of numerous experimental, analytical, and computational approaches to determine the macroscopic thermal behaviour of composite materials. This chapter, is focused on the Multiphysics (coupled-physics computational) approaches. The choice of the representative geometry of the model adopted to represent the composite microstructure, heat conduction can be treated as a one-, two-, or three-dimensional phenomenon. Many factors affect the effective thermal conductivity of composites. Here, chose a cube of $100\mu\text{m}\times 100\mu\text{m}\times 100\mu\text{m}$ as the Representative Volume Element in glorious 3d as the matrix and an array of cylindrical micro-rods as the graphene filler or element.

According to Cruz [17], theoretically, the temperatures, thermal conductivities, relative volume amounts, geometries, and spatial and size distributions of the constituent phases affect the thermal characteristics of the composite. However, because actual manufacturing processes of composite materials are often characterised by imperfections from process variability, in practice the effective conductivity also depends on the interfacial thermal resistance between the phases and the porosity (void) content. In addition, analytical and computational analyses become more cumbersome when there exist more phases that are anisotropic (with tensorial transport properties), and when there

are nearly-touching or touching inclusions (fibres or particles) in the composite. In the context of a more realistic representation of physics of the microstructure, the analyses implicitly take into account the temperature dependence of the effective conductivity, by considering temperature dependent properties of the individual phases. The most important intrinsic properties affecting the behaviour of composite is the temperature. It determines the overall behaviour of the resulting material owing to its sensitivity to small change in temperature of its environment.

The chapter is organized as follows. The theory of thermal conductivity of carbon material is explored in section 1. In section 2, the state of the art experimental approaches available are presented. The Multiphysics method is presented in section 3 to bring the reader up to speed with these robust techniques. The coupled-physics method is considered from the perspective of electric current induced transient and stationary heat transport in the composite in the time domain in section 4. The concluding remarks and the future research outlook on composite science and technology are presented in section 5.

2 Theory of thermal conductivity

There is a growing search for material with superior thermal, electrical conductivity for next generation of integrated circuits and three-dimensional electronics, optoelectronic and photonics. In other applications such as thermoelectric energy conversion requires a material that have a strongly suppressed thermal conductivity.

The thermal property of a material here refers to its ability to conduct heat from one point to another, depends on the atomic structure of the substance. Also, the thermal properties of material changes when they are structured on a nanometre scale. The Nano-architecture or transformation of nanostructured material into a nanowire, make the nanowire material not to conduct heat as well as in bulk crystal owing to increased phonon-boundary scattering or changes in the phonon dispersion. A large infinitely intrinsic thermal conductivity exotic behaviour has been displayed by two-dimensional and one-dimensional materials.

2.1 Determination of Thermal conductivity of composite

The determination of thermal conductivity of composite materials as highlighted in the overview of the chapter, is essential for the understanding the extent of heat removal or retention in solid, liquid or gas. Here presented, are very recent methods of determining the thermal conductivity of solid, liquid and gaseous substances. The key methods are presented in the section as follows:

2.2 Instrument available for measuring thermal conductivity

There are range of thermal conductivity measurement devices but, our focus is on the tools that are relevant to the coupled-physics modelling approach that mimic our computational technique adopted.

2.2.1 Modified Transient Plane Source (MTPS)

The modified transient plane source method is a time dependent technique for measuring the thermal conductivity of solid, liquid and gaseous substances. The experimental setup of the technique and the response voltage-time² as shown in the setup of the modified transient plane source thermal conductivity measurement technique in Fig. 1. The method is based on a Guard ring technology characterised without Regression analysis, additional thermal properties and sample preparation in other measurement techniques.

The setup operation start with an applied current is simultaneously producing heat from the sensor coil and guard ring. The guard ring and the insulator support a dimensional transient heat transfer from the coil to the sample (Liquid, gas, solid or powder). The rate of temperature increase is monitored by the voltage drop of the primary sensor coil which is calibrated to the temperature change. The thermal conductivity is proportional to the rate of increase in temperature. The lower the thermal conductivity of the sample the steeper the rise in temperature and vice versa as shown in the voltage (mV) and square response in Fig. 1. Unlike other transient methods, these method is developed with standardised timing and power parameters. Eliminating the ambiguity in obtaining repeatable results among laboratories and removing operator's potential bias.

This experimental method is based on resistive Joules Heating in only 1 dimension. The Multiphysics methods can be employed to leverage and extend the measurement and design of such equipment from the concept phase to fully experimental equipment without building the prototype during the development phase. The readers interest in MTPS experimental technique take advantage of the work of the following authors [18–20]

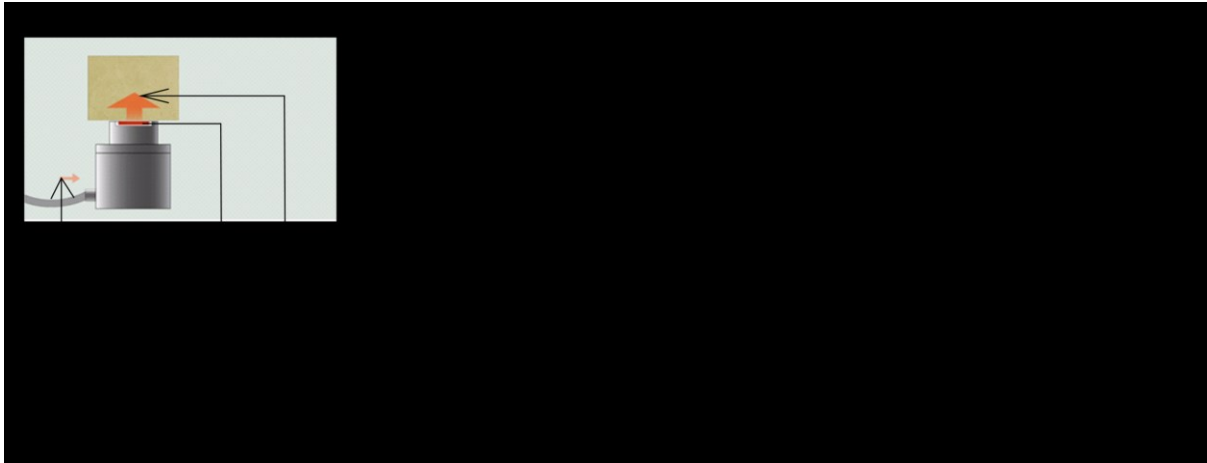


Fig. 1 (A) setup of the modified transient plane source thermal conductivity measurement technique showing the resistive heating source the sample and the direction of heat flow; (B) is a typical response curve showing the voltage (mV) and temperature as a function of the square of the heating time with 2 distinct region for low and highly conductive material sample [18–20].

2.2.2 Laser Flash Diffusivity-thermal conductivity method

The laser flash method measures length of the sample and taking its square and dividing it by the half-time rise of the sample and multiplying the result with a factor 0.13879, as seen in the diffusivity eq. 1. The thermal diffusivity is determined from thermal diffusivity (α), specific heat capacity (C_p) and density (ρ). The laser heats the sample to a couple of degrees. The infrared detector on the top measures or looks at the heat signature of the pulse of the laser light wave as it propagates through the materials. The instrument measures the time response (half-time) of the heat waves as it passes through the materials (sample). The time is multiplied by the C_p , α and ρ of the material (sample) to give the thermal conductivity as seen in the thermal conductivity eq. 2. The method is useful for estimating the time required for heat to travel through a material either through phonon in nanostructure carbon material or through lattice electron vibration in metals as shown in the laser setup in Fig. 2A. The typical output of laser flash thermal conductivity technique is shown in Fig. 2B. The temperature differential at half the exposure time $\Delta T_{\frac{1}{2}}$ is read off with its corresponding half time $t_{\frac{1}{2}}$. The value is used to compute the value of α in Eq. (1).

The sample is placed in the sample holder and irradiated by laser and the lens converges the beam of laser to a specific diameter as shown in the varying diameter lens in Fig. 2C (25.4 mm), Fig. 2D (10 mm) and Fig. 2E (3 mm). The three diameters are proportional to the diameter of the sample holder. The varying lens diameter is to accommodate varying test sample diameters. A typical temperature rise measurement trajectory is compared with a model as shown in Fig. 2F. Interested readers can refer a detail treatment of the measurement techniques in [21–24]

- Fast techniques

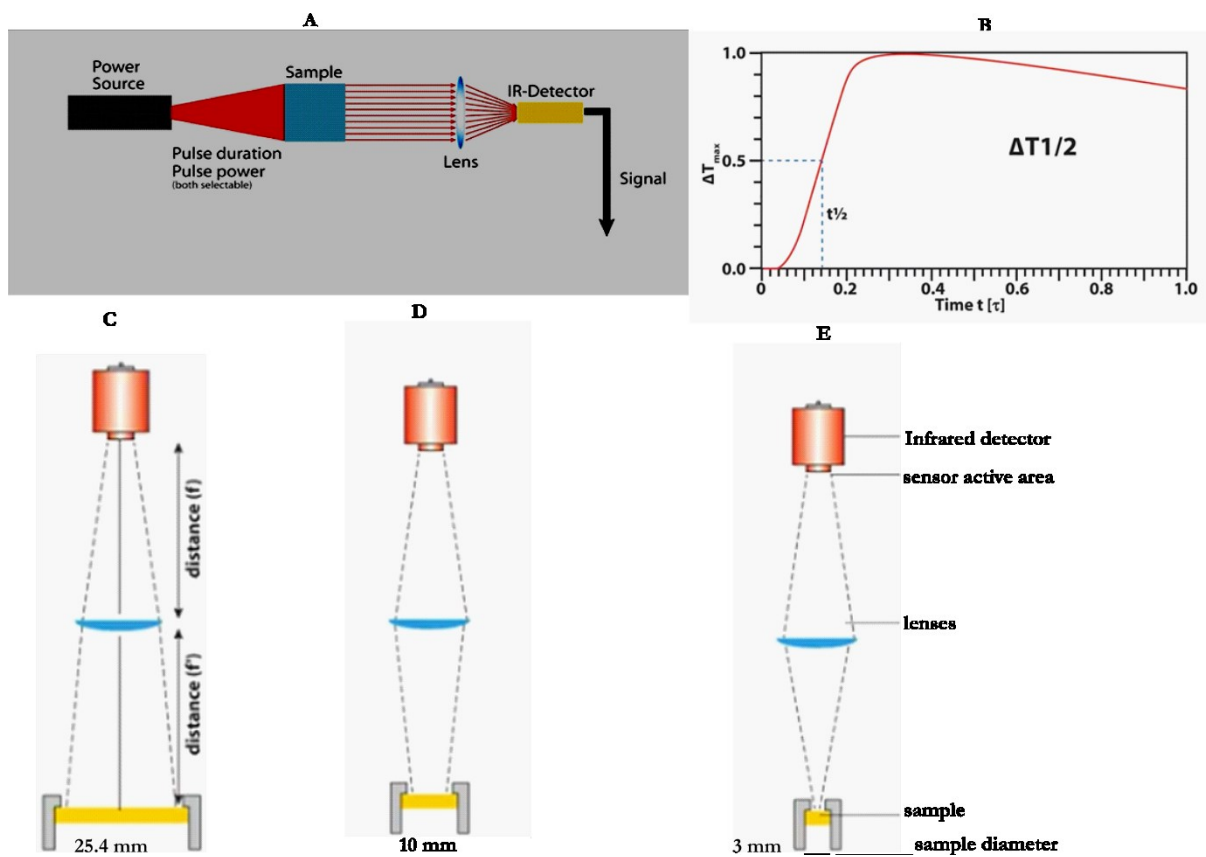
- Non-destructive
- Relatively easy sample preparation

$$\alpha = \frac{0.13879L^2}{t_{\frac{1}{2}}} \quad (1)$$

α is thermal Diffusivity of the sample; L is the sample height; $t_{\frac{1}{2}}$ is the half time rise

The thermal conductivity is determined as seen in thermal conductivity eq. 2

$$\lambda = \alpha C_p \rho \quad (2)$$



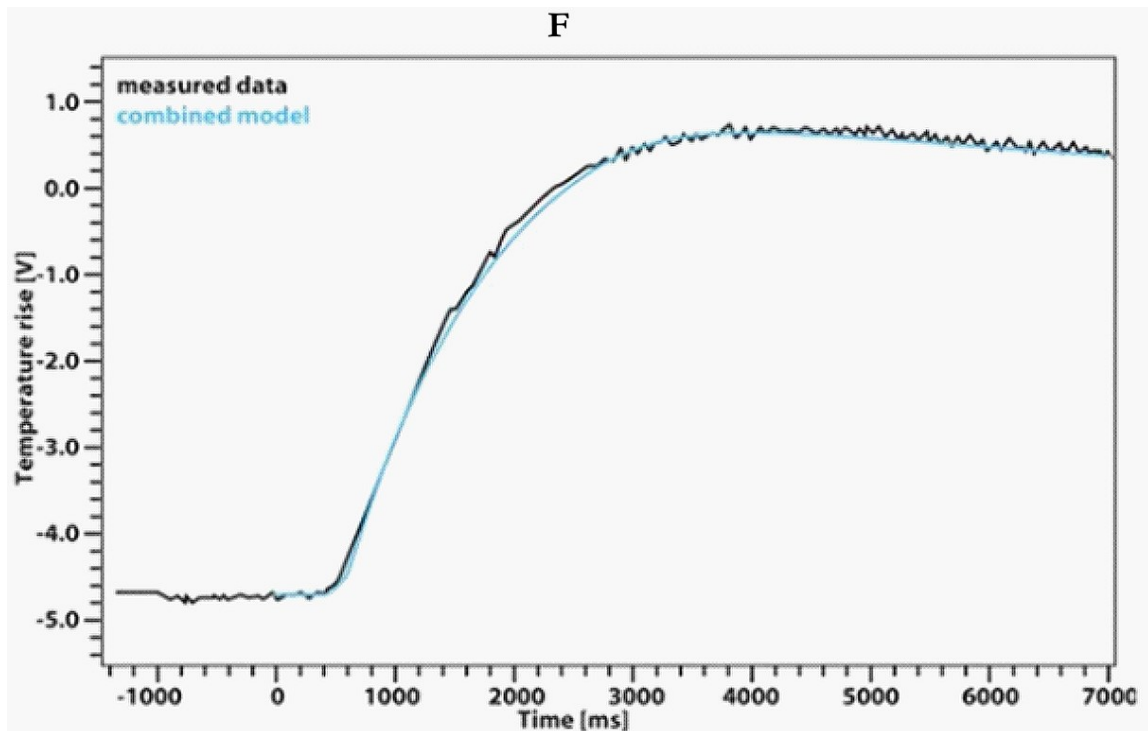


Fig. 2 (A) Laser Flash thermal diffusivity-conductivity setup method for measuring thermal conductivity; (B) The change in temperature response time of sample material to pulse current change; (C) 25.4 mm Lens positioning relative to the infrared and sample; (D) 10 mm Lens positioning relative to the infrared and sample; (E) 3 mm Lens positioning relative to the infrared and sample; (F) measured data of the combined model temperature rise trajectory of a typical sample [21–24].

3 Multiphysics methods

3.1 Multiphysics definition

Multiphysics is computation modelling paradigm that enables scientist and engineers to combine or couple different physical phenomena (e.g. physics-heat transfer, electrochemistry, structural mechanics, fluid flow, optics, Alternating and direct current) to capture the simultaneous happenings of several phenomenal behaviour of a system. The tool or techniques captures the true essence of the multiple behaviour occurring in a real system. The traditional way of engineers and scientists must make assumptions in order to be able to realize their design ideas, has radically been transformed and redefined by Multiphysics. Using Multiphysics possible as time progresses during the modelling process for these assumptions are being refined and, in some cases, even eliminated, to obtain more accurate and realistic results. Multiphysics provides the toolset to eliminate

assumptions. There are several computer-based software applications for implementing this solution paradigm. The software application includes but not limited to;

- ❖ COMSOL Multiphysics
- ❖ ANSYS Multiphysics
- ❖ Open FOAM
- ❖ FEA Tool Multiphysics

The selection of software tools depends on many factors such as affordability, ease of use, learning curve and users support and its ability to handle large 3d complex geometry (model), CAD supports, integration of all tools within the same platform or integrated development environment. One of the software application that carry most of these benefits with it is COMSOL Multiphysics.

COMSOL is an integrated simulation environment, designed with real-world applications in mind from ground up. The numerical engine is based on Finite Element Modelling. The ultimate goal of all simulation tool is to of course mimic, as closely as possible, effects that are observed in real world. These physical phenomena occur in an engineering and scientific perspective. In addition, to achieve this, there is a need of Multiphysics; that is the availability of multiple scientific models that include the phenomena that are of interest. These physics include acoustics, electromagnetics, chemical reactions, mechanics, fluid flow, and heat transfer. The real world combines all these effects, the solution simulation environment should also be able to reflect or capture these effect in its built. This is what COMSOL seeks to deliver, and it is done in an easy-to-use workflow and interface with the sole purpose of making scientists and engineers more productive in their day-to-day work design and research [25–28].

There are several studies reported on the effective thermal conductivity of composite using the Multiphysics approach. Theoretical and empirical models have been proposed to predict the effective thermal conductivity by different authors [29–31], Milton and these authors [32–37], Furmanski [38] and Mirmira and Fletcher [39]. In another study, Eian and Deissler investigated the thermal conductivity of filled polymer [5,40,41]. This work was extended by Wakao and Kato[6], specifically for a cubic or orthorhombic array of uniform spheres of particles in contact with themselves. The effect of particle or filler contact with a matrix using a 2-dimensional model of a composite was investigated by Shonnard and Whitaker [42], using a global equation with an integral method for heat transfer. In a similar study, Auriault and Ene [43,44] investigated the effect of interfacial thermal barrier on the thermal conductivity and the shape and structure of the macroscopic heat transfer equations. A finite element method was used to unravel the heat conduction of periodic distribution of filler in composite material. The significance of these

investigation in conjunction with the work of Ramani and Vaidyanathan [45] is the coupling of the effect of microstructural characteristics which include filler aspect ratio, interfacial thermal resistance, and volume fraction and filler dispersion to determine the effective thermal conductivity of composite. The filler particles studied by these authors are parallelepiped and spherical in shape. An alternative numerical tool was used by Liang [46] to study the heat transfer in hollow-glass-bead filled polymer composites. The effective thermal conductivity dependence on the content and size of the hollow-glass-bead was revealed. A molecular and mechanistic approach was used to study the effective thermal conductivity of polypropylene/ hollow-glass-bead was estimated [47]. The molecular and mechanistic method was based on Lattice Monte Carlo (LMC) and finite element analyses. The effective thermal conductivity of sintered metallic hollow spheres shapes was studied by Fiedler et al. [47,48]. The LMC approach was extended to incorporate temperature dependence of thermal conductivity and specific heat in transient thermal analyses [49].

3.2 Electromagnetic heating

Electromagnetic heating is an emerging heat transfer technique aimed at direct heating of material at the atomic or molecular level using electromagnetic wave spanning the entire electromagnetic spectrum (Gamma ray - Radio wave). The electromagnetic heating is a relatively new technique and has been successfully applied in enhanced oil recovery [50–58]. These studies have proven to be very effective in heating the specific material required, unlike conventional heating method that heats the bulk material including non-desirable part like the container with the sample. The current challenges with these technique is that the mass and heat transfer interaction between the material and its surroundings are still not fully understood.

There are currently four electromagnetic heating methods viz;

- Resistive Joule's heating
- Laser Heating
- Induction heating
- Microwave heating

However, here we focus on resistive Joule's heating as follows. This is because of space and the treatment of the other electromagnetic heating is beyond the scope of this chapter.

3.3 Resistive Joules heating

The resistive heating occurs when electric current is applied to a material along a potential, heat is produced as result of the material resistance to the flow of electron through it. It could also be described as a process where the energy of an electric current is converted into heat as it flows

through a resistance. In particular, where electric current flows through a solid or liquid with finite conductivity, electric energy is converted to heat through resistive losses in the material. The heat is generated on the atomic scale when the conduction electrons transfer energy to the conductor's atoms by way of collisions. The response to the flow of current is because all matter is composed of atoms containing positively charged nuclei and negatively charged electrons. The positive and negatively charges produce and respond to the stimuli of electromagnetic field, as seen in the Maxwell's set of equations (3)-(6), expressed in the macroscopic form as follows;

$$\nabla \times E = -\frac{\partial B}{\partial t} \quad (3)$$

$$\nabla \times H = J + \frac{\partial D}{\partial t} \quad (4)$$

$$\nabla \cdot D = \rho_v \quad (5)$$

$$\nabla \cdot B = 0 \quad (6)$$

The electrical material properties of the composite is computed by the Finite element modelling method using equations (7) and (8) which is for homogeneous linear isotropic materials. The electric displacement D is the product of the permittivity and the Electric field as seen in the electric displacement equation (7). The magnetic field is the product of the permeability and the magnetisation as seen in the magnetic field equation (8);

$$D = \epsilon E \quad (7)$$

$$B = \mu H \quad (8)$$

The Eq. in 3 in the Maxwell's equation set is also referred to as the Faradays Law of Induction and state that a time dependent change in the local magnetic field will produced an electric field. In simple term, wherever there is a magnetic field, there exists and electric field perpendicular to the direction of the magnetic field.

Equation 4 is an extension to Ampere Law, which state that a steady electric current produces a magnetic field. The contributions of Maxwell to equation was the addition of a displacement current term $\frac{\partial D}{\partial t}$, which defines and explains the production of the time varying electric field and the steady current by the magnetisation field. The Gauss Law is represented by Eq. 7 which state that electric field is produced by electric charge. The fourth equation is also known as the Gauss' Law for Magnetism and state that there are no analogues of electric charge for magnetic fields.

3.4 Implementation of resistive heating to evaluate thermal conductivity of composite

The implementation of the coupled-physics resistive heating of a graphene-starch composite is demonstrated here involving a 9-step process from defining the model on a napkin-paper with all the geometry, with a clearly marked boundaries and domains to result and post processing. The 9 steps are as follows;

3.4.1 COMSOL 5.3 Model Wizard

The model Wizard provides some guided steps in selecting the spaced dimension, physics type and study for the modelling task. The steps involved in the setup of the composite model in 3d are described briefly as follows;



1. Open the Model Wizard and select the 3Model wizard tab () and click the 3D spatial dimension in the select space dimension window
2. In the Select Physics panel, click on the forward arrow in front of heat transfer in the select Physics window to expand the physics.
3. Click on the forward arrow in front of Electromagnetic heating to expand.
4. Right-click on the Joule Heating tab and select Add physics.
5. Click the Study arrow to open the Select Study panel.
6. Select Time dependent study and click “Done”.

This will exit the Model Wizard, COMSOL will populate the model builder with global definition, components, Electric current, Heat transfer in solids, Multiphysics, Mesh and results interface. The model Wizard setup steps are summarised in Model Wizard Setup windows A-H shown in Fig. 3.

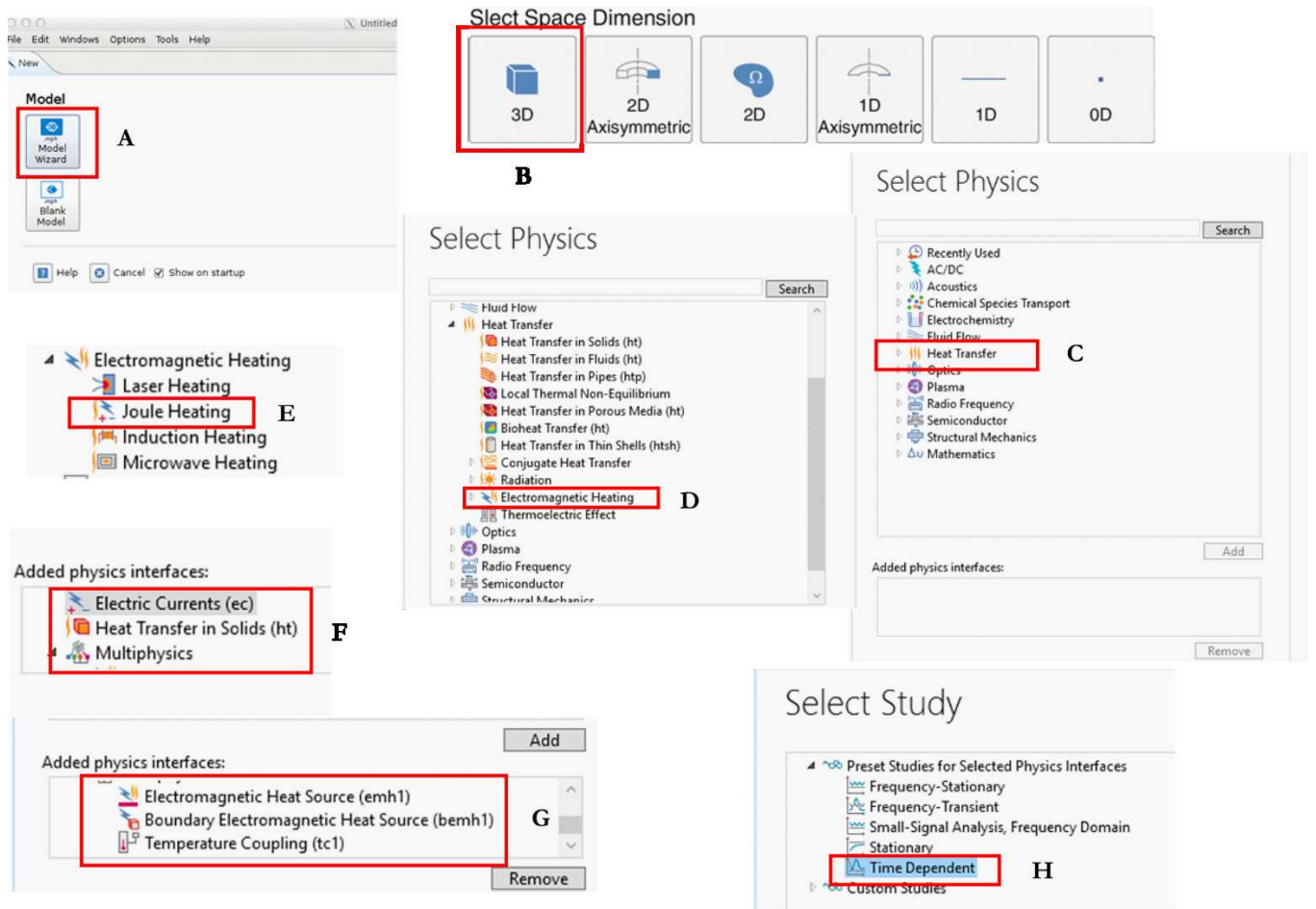


Fig. 3 Model Wizard Setup windows A-H

The red rectangular marker and the letter in front indicate and shows the work flow as shown in the model wizard window in Fig. 3. The can be started from the desktop or from the start bar. Double-clicking on the COMSOL Multiphysics short-cut on the desktop, launches integrated development environment.

3.4.2 Model definition

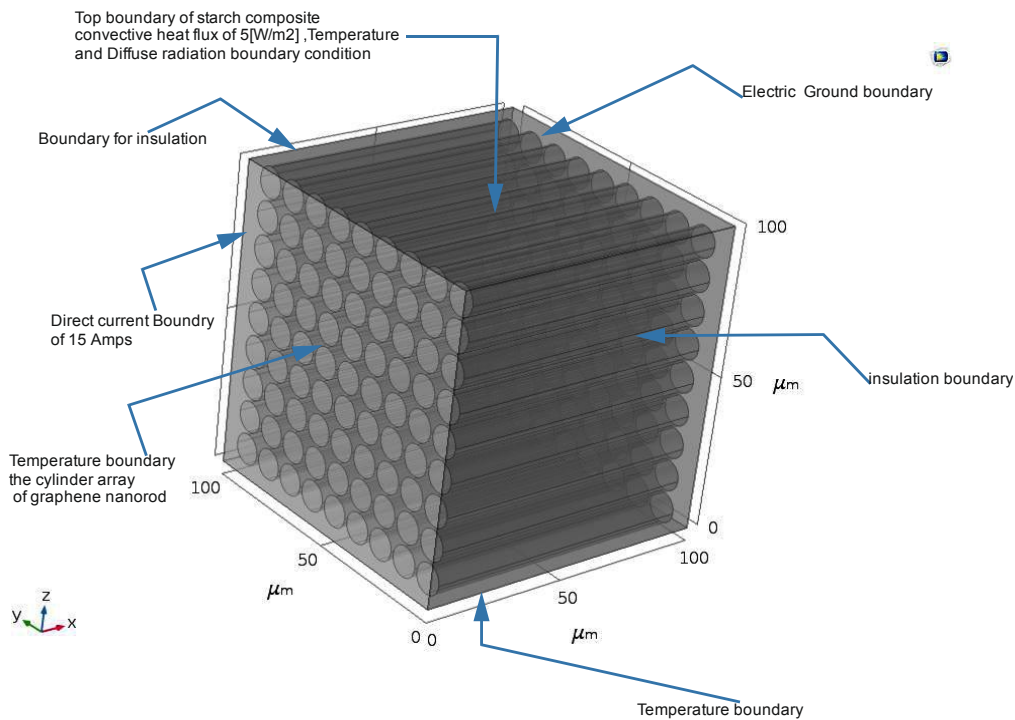


Fig. 4 Model geometry definition of all the boundaries and domains of the conditions applied in realising the solution of the coupled Direct Current, heat transfer in solids and Multiphysics electromagnetic heating

The model is represented in a cube of dimension $100 \times 100 \times 100 \mu m$ with the graphene fibres of dimension of radius $5 \mu m$ and height $90 \mu m$ and 3d array of $9 \times 9 \times 9$, encapsulated in starch matrix. The electrical and thermal boundary conditions are described as shown in the model definition in Fig.4. The two physics (Electrical and thermal are couple with the electromagnetic field), are solved using the finite element modelling discretisation using commercial COMSOL Multiphysics software package. The Maxwell equation set (1)-(4) with the 3-dimensional Fourier equations are solved to obtain the material properties of the composite.

3.4.3 Global definition and parameter specification

The global definition step involves the inputting the thermophysical property values obtained from experimental modelling in the parameter window in the global definition tab of the model builder tree. The parameter specification definition is very handy especially when a what-if analysis or sensitivity study or parameter sweep is desirable. The property values are assigned in the material definition phase to create new material not present in the COMSOL material database. We defined the electrical thermal property values for starch and graphene in the parameters window as shown in the global definition tab parameter window in Fig. 5.

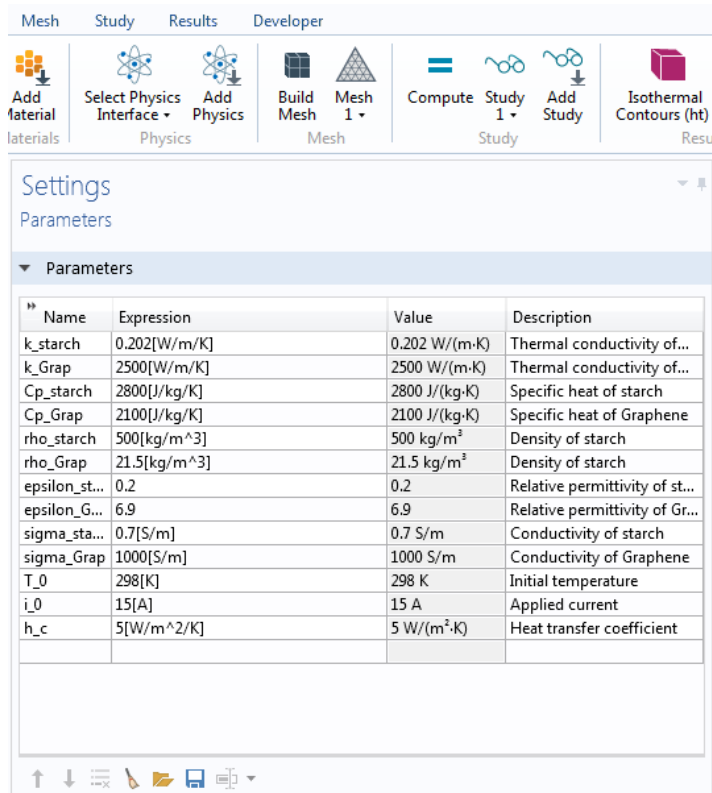


Fig. 5 Global definition tab parameter window

3.4.4 Model setup

The model setup provides the tools for creating geometry of a model. A block tool was used to create the starch block and the cylinder primitive was used to draw the graphene fibre. The array modify tool was used to create a rectangular array of the graphene fibre dispersed in the starch matrix. The assembly tool was used to combine the starch block and the graphene cylinder array as a single composite entity. The block, graphene, array and assembly setting in the geometry creation node in the model tree window is shown in the model geometry setting in Fig. 6

3.4.5 Geometry creation

The drawing of primitive in COMSOL can either be by one, two or three dimensions. The drawing of geometry in 1 and 2 dimensions involves the use of 2D tools like point, lines, rectangles etc. In 3 d modelling of geometric entities, the shapes can be created directly using existing and pre-programmed geometric primitives such as spheres, cylinder, blocks, torus etc. A complex shape can be modelled using Boolean modify tools such as union, subtract, array etc. The second method of drawing 3d shapes is using 2d shapes in a work plane and transforming the shape using transformation tools such as revolve, extrude, sweep etc.

The 3d shape can be imported as a Stereolithographic file (STL), using COMSOL geometry livelink tools such as Live link for Solidworks, Inventor etc. In this chapter, the model of the composite

was created using the existing pre-programmed geometric primitives as shown in the 3-step window in model setup Fig.5.

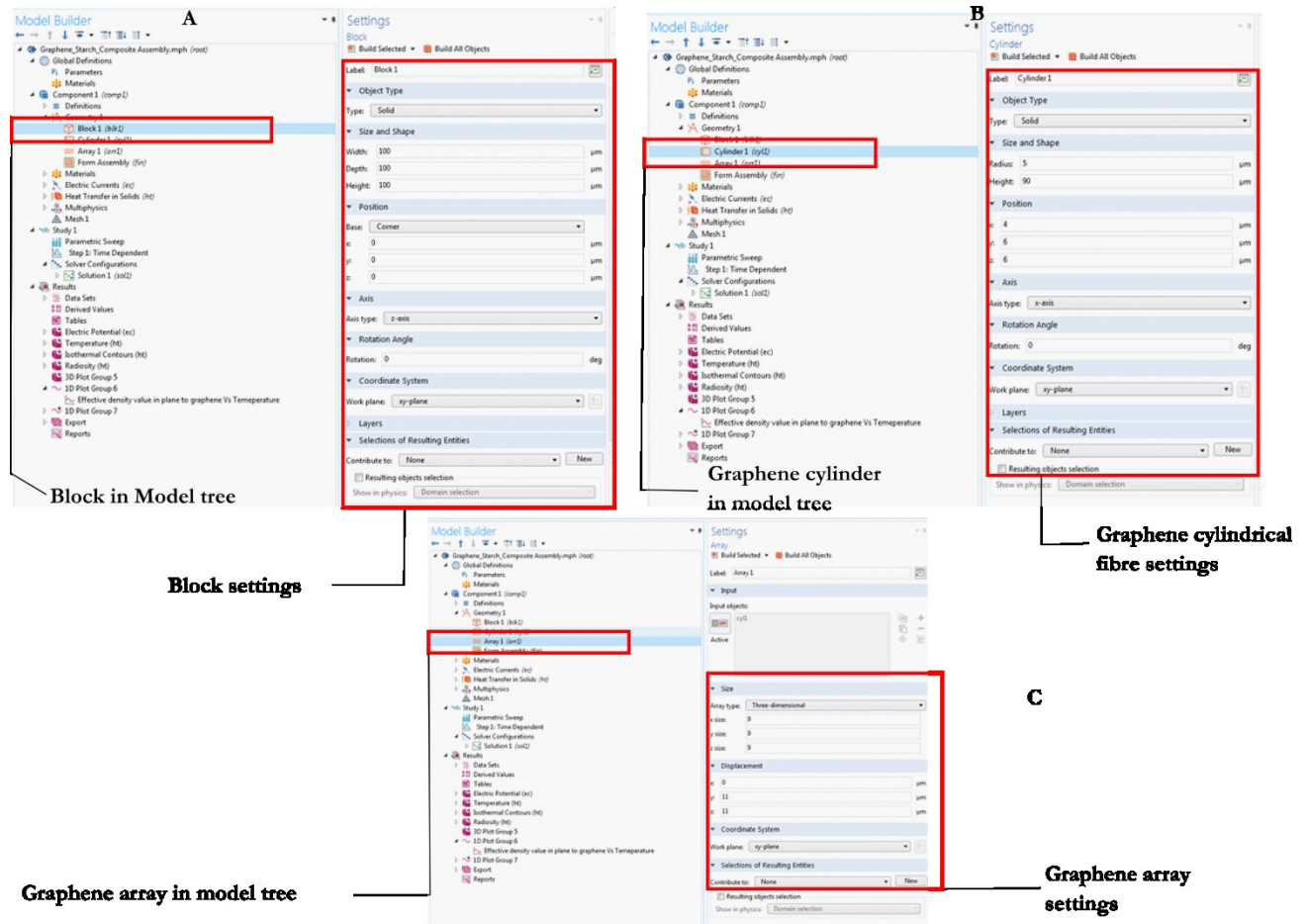


Fig.6 Model setup window; A: Starch Block and block primitive settings; B: Graphene fibre cylinder and the cylinder setting; C: Graphene array and settings

3.4.6 Material definition and modelling

The material tab in the model builder window, the graphene and starch materials are not available in COMSOL material database. The Blank Material option was used to selected from the 4-available option as shown in the material short-cut selection window as shown the Material options and special exotic materials in Fig. 7. Both materials were created as user defined by specifying the density, specific heat capacity, thermal conductivity and the electrical conductivity and permittivity of starch and graphene for the set of the Maxwell (eq. 1-4). They provide an array of materials from the General Material Library, Built-in, special materials for selected exotic physics such as AC/DC, batteries and Fuel Cells etc.

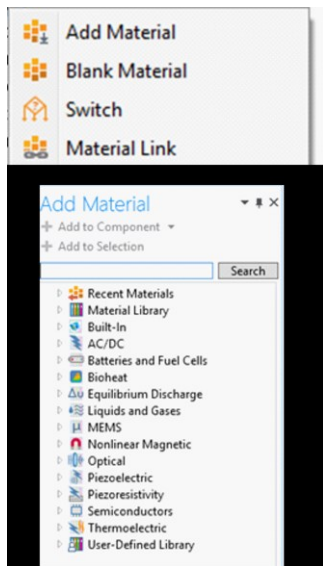


Fig.7 Material options and special exotic materials for specialised physics in COMSOL Multiphysics

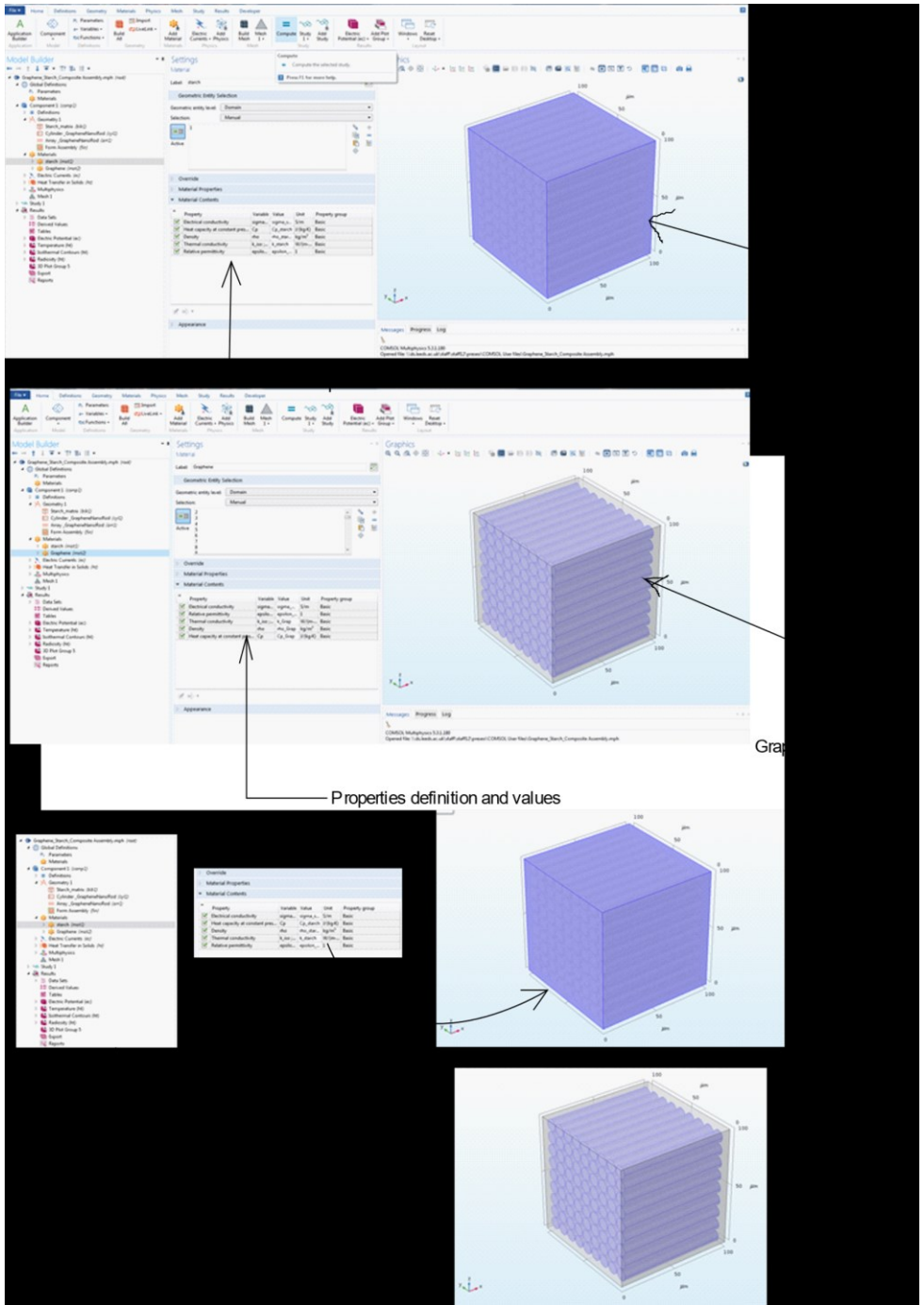


Fig. 8 A detail procedural steps for creating a user defined graphene and starch material in COMSOL

The advantage of COMSOL as a modelling tool is that it provides several opportunities to innovate and create new materials for research and development as shown in Material options and special exotic materials for specialised physics in COMSOL Multiphysics (Fig. 7) and the procedural steps (Fig. 8). In Fig.8 the shows in graphic detail distinct domain assigning of user defined starch and graphene properties. The starch domain is distinctively isolated from the graphene array as shown in the first and second windows.

3.4.7 Physics and Multiphysics coupling definition on domains and boundary

3.4.7.1 Electric current physics node

The electric current physics is used to compute the electric field, current and the potential distributions in conducting media under conditions of negligible inductive effects, in which case the skin depth is much larger than the graphene-starch composite. The current density (J) in 3-dimensional space is related to the electric volumetric heat source ($Q_{j,v}$) as seen in the current density Eq. (7).

The current conservation sub node provides the model equation for the electric potential and provides a setting window for defining the electrical conductivity, electric field displacement and the relative permittivity of the graphene-starch composite as seen in the transient Ohm's Law Eq. (8). The current density (J) relate the electric field (E) to the electrical conductivity (σ) of the composite to the relative permittivity (ϵ_r). The applied potential (ΔV) with the Laplacian operator (Δ) is related to the electric field as seen in the electric field Eq. (9)

The equations representing the boundaries are as follows;

$$\nabla \cdot J = Q_{j,v} \quad (9)$$

$$J = \left(\sigma + \epsilon_0 \epsilon_r \frac{\partial}{\partial t} \right) E + J_e \quad (10)$$

$$E = -\nabla V \quad (11)$$

3.4.7.2 Electric Insulation BC, All boundaries except 1 & 6 (Fig. 4)

The electrical insulation provides a means of specifying boundaries which do not require current to flow through and discontinue the electrical potential difference as shown in the Electric current physics boundary conditions in Fig. 9 and expressed mathematically as seen in the dot product of the normal vector (n) and the current density (J) conservation Eq. (12).

$$n \cdot J = 0 \quad (12)$$

3.4.7.3 Initial values

COMSOL solvers require an initial value for the electric potential for a transient simulation or iterations or an initial guess for a nonlinear solver as seen in the electrical potential difference conservation Eq. (13).

3.4.7.4 Ground Boundary condition on face 6 (Fig. 4)

The ground boundary provides a face 6 in the composite for the COMSOL solver to send or distribute the current at a zero potential as seen in the electrical potential difference conservation Eq. (13).

$$V = 0 \quad (13)$$

3.4.7.5 Terminal Boundary conditions on face 1 (Fig.4)

The terminal is a boundary or domain condition in the composite on face 1 for connection to external circuits to transmission lines with a specified voltage or current as seen in the terminal Eq. (14). The electric current physics is defined as shown in the electric current physics boundary conditions in Fig. 9.

$$\int_{\partial\Omega} J \cdot ndS = I_0 \quad (14)$$

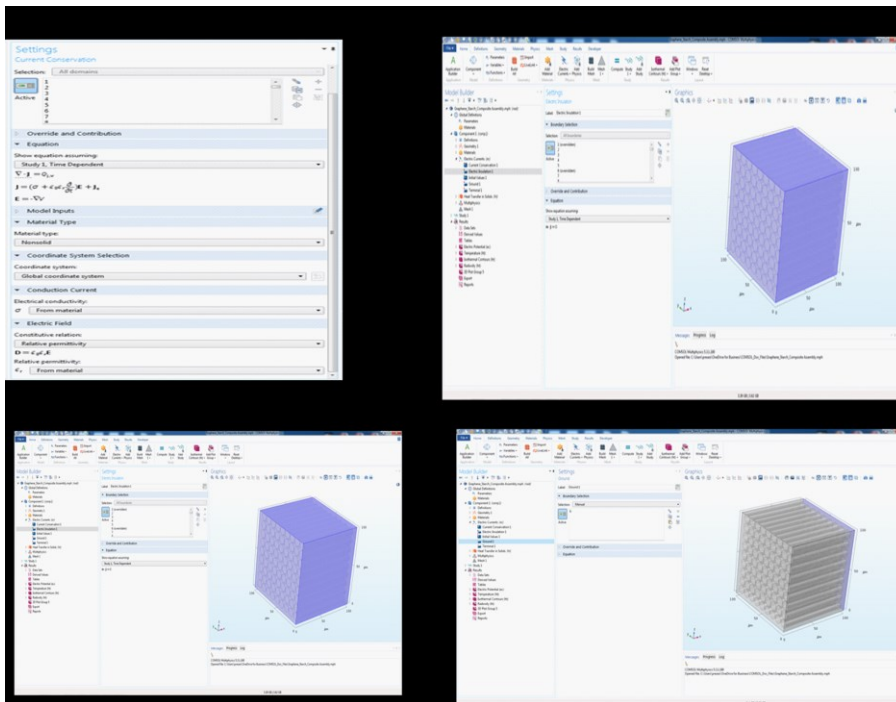


Fig. 9 Electric current physics boundary conditions

3.4.8 Modelling Heat Transfer in Solids Physics

3.4.8.1 Conduction in Solids-all boundaries

Modelling the heat conduction in the solid graphene-starch composite is a 3 dimensional transient modelling of Fourier Law, with materials properties of composite solid densities ($\rho_{graphene}$ and ρ_{starch}), specific heat capacities at constant pressure ($C_{pgraphene}$ and $C_{pstarch}$),

and the solid thermal conductivities ($k_{graphene}$ and k_{starch}). The Finite element techniques computes the overall material properties from individual materials properties (graphene and starch). The velocity field \mathbf{u} is the velocity field defined by the translational motion when the part of the composite move as a result of the electric and magnetic field applied at the electrical terminal (Fig. 9). The heat source from the electric current density drives the heat conduction (Q and Q_{ted}) in the composite as seen in the Fourier Eq. (15). The heat flux is convective heat flux in the as seen in the heat flux thermal conductivity Eq. (16). The implementation of the heat transfer by conduction solids is as shown in the heat transfer in solid physics boundary conditions in Fig. 10. The Laplacian operator ∇ is defined as;

$$\nabla = \frac{\partial^2}{\partial x^2} + \frac{\partial^2}{\partial y^2} + \frac{\partial^2}{\partial z^2}$$

$$\rho C_p \frac{\partial T}{\partial t} + \rho C_p \mathbf{u} \cdot \nabla T + \nabla \cdot \mathbf{q} = Q + Q_{ted} \quad (15)$$

$$\mathbf{q} = -k \nabla T \quad (16)$$

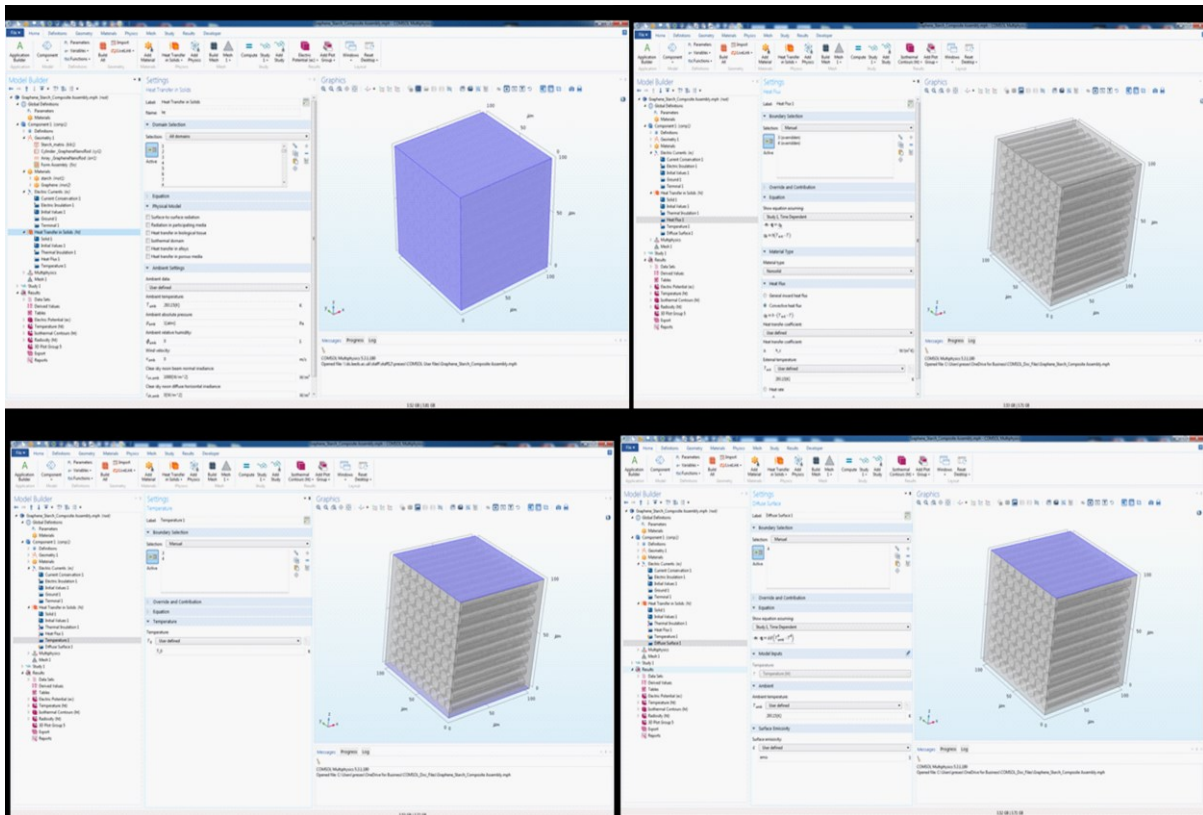


Fig. 10 Heat transfer in solid physics boundary conditions

4 Multiphysics interface

A Multiphysics system consists of more than one component governed by its own principle(s) for evolution or equilibrium, typically conservation or constitutive laws.

The Multiphysics interface was used to combine or couple the electric current interface and the heat transfer in solids interface as single and seamless electromagnetic Joule heating interface, through a 2-way coupling () as seen in the electromagnetic heating Eq. (17).

$$\rho C_p \frac{\partial T}{\partial t} + \rho C_p \mathbf{u} \cdot \nabla T = \nabla \cdot (\mathbf{k} \nabla T) + Q_e \quad (17)$$

The Multiphysics classification in the composite system and many other such systems could be whether the coupling occurs in the bulk (e.g., through source terms or constitutive relations that are active in the overlapping domains of the individual components) or whether it occurs over an idealized interface that is lower dimensional or a narrow buffer zone (e.g., through boundary conditions that transmit fluxes, pressures, or displacements). The approach is hybrid with respect to the composite model and the details of the implementation is set out as shown in Multiphysics electromagnetic heating coupling settings in Fig. 11.

There are other typical examples of bulk-coupled Multiphysics systems with their own extensively developed literature including radiation with hydrodynamics in astrophysics (radiation hydrodynamics, or RHD), electricity and magnetism with hydrodynamics in plasma physics (magnetohydrodynamics, or MHD), and chemical reaction with transport in combustion or subsurface flows (reactive transport) [59]. On the other hand, typical examples of interface-coupled Multiphysics systems are ocean–atmosphere dynamics in geophysics, fluid–structure dynamics in aeroelasticity, and core–edge coupling in tokamaks [59–61]. Beyond these classic Multiphysics systems are many others that combines important structural features. The hybrid approach is summarised as shown in the Multiphysics electromagnetic heating coupling settings in Fig. 11 in the COMSOL Multiphysics development window.

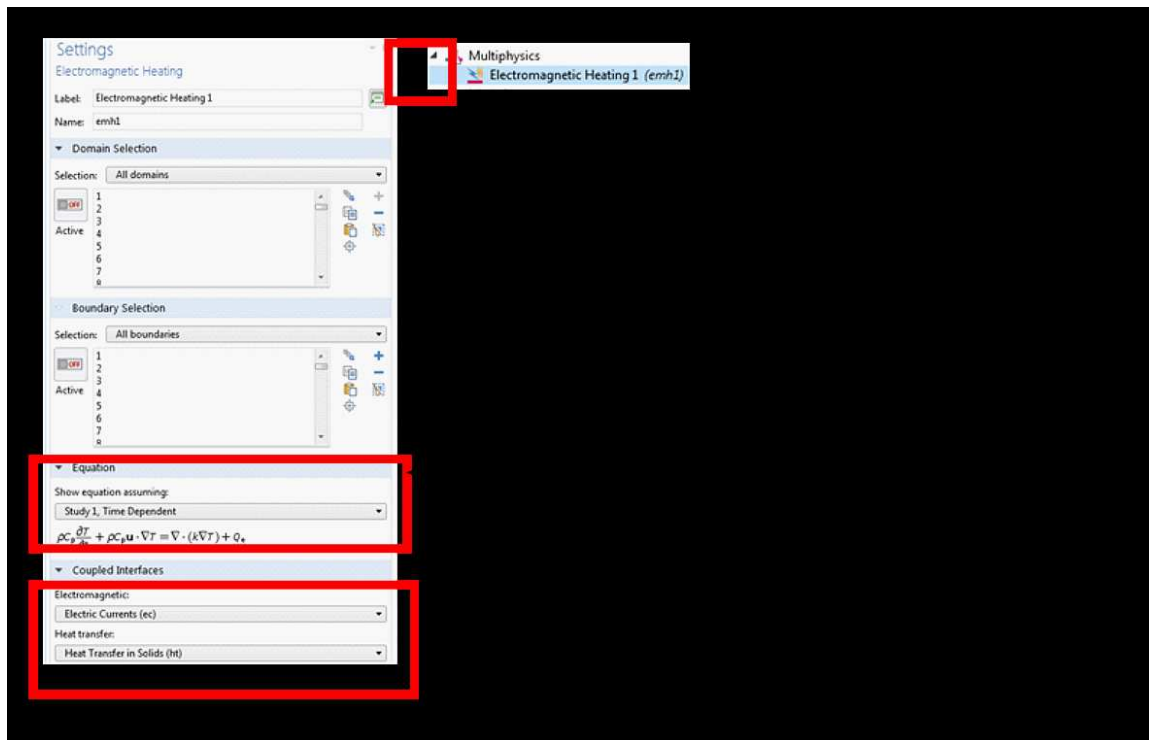


Fig. 11 Multiphysics electromagnetic heating coupling settings

4.1 The mesh

The meshing discretises divides the composite (graphene cylinders array and the starch) domains as shown in the meshing settings in Fig. 12. The mesh approach was based on a quick solution (not a fine mesh) to the material properties of the graphene composite. A 1s transient simulation (very short simulation time of 1 s) was set in the solver time setting to reduce the computational burden and for a quick convergence of the solution.

In COMSOL, the *mesh* node provides the option to split the geometry into discrete mesh elements. This helps to simplify complex geometries for solving.

Finer meshes have a greater number of elements and therefore result in solutions with a greater resolution. Coarser meshes can be used to speed up solving times. Note that it is important to weigh up the trade-off between high accuracy and time taken to compute the solution when applying a very fine mesh to a geometry.

To create a mesh, click either, the **physics-controlled mesh** or **user-controlled mesh**, for defining the size of the mesh elements.

The **physics-controlled mesh** option was adopted to allows picking from nine different pre-defined mesh sizes, from extremely fine up to extremely coarse. In this simulation, an extra coarse mesh provided a quick solution to the simulation of the composite. The extra coarse mesh is an option in the element size under the physics-controlled mesh sequence type as shown in mesh settings in Fig.12. The mesh consists of 314514 Tetrahedral elements, 230904 triangular elements, 64200 edge elements and 5840 Vertex elements. The average element quality is 0.7288, a good value for an extra coarse mesh. The mesh is adequate for the transient solution to the composite

material property values. A more refined mesh will put a strain on the computational resources and the solution may not converge. Hence, an extra coarse mesh provides a reasonable result and convergence for the computational resource available.

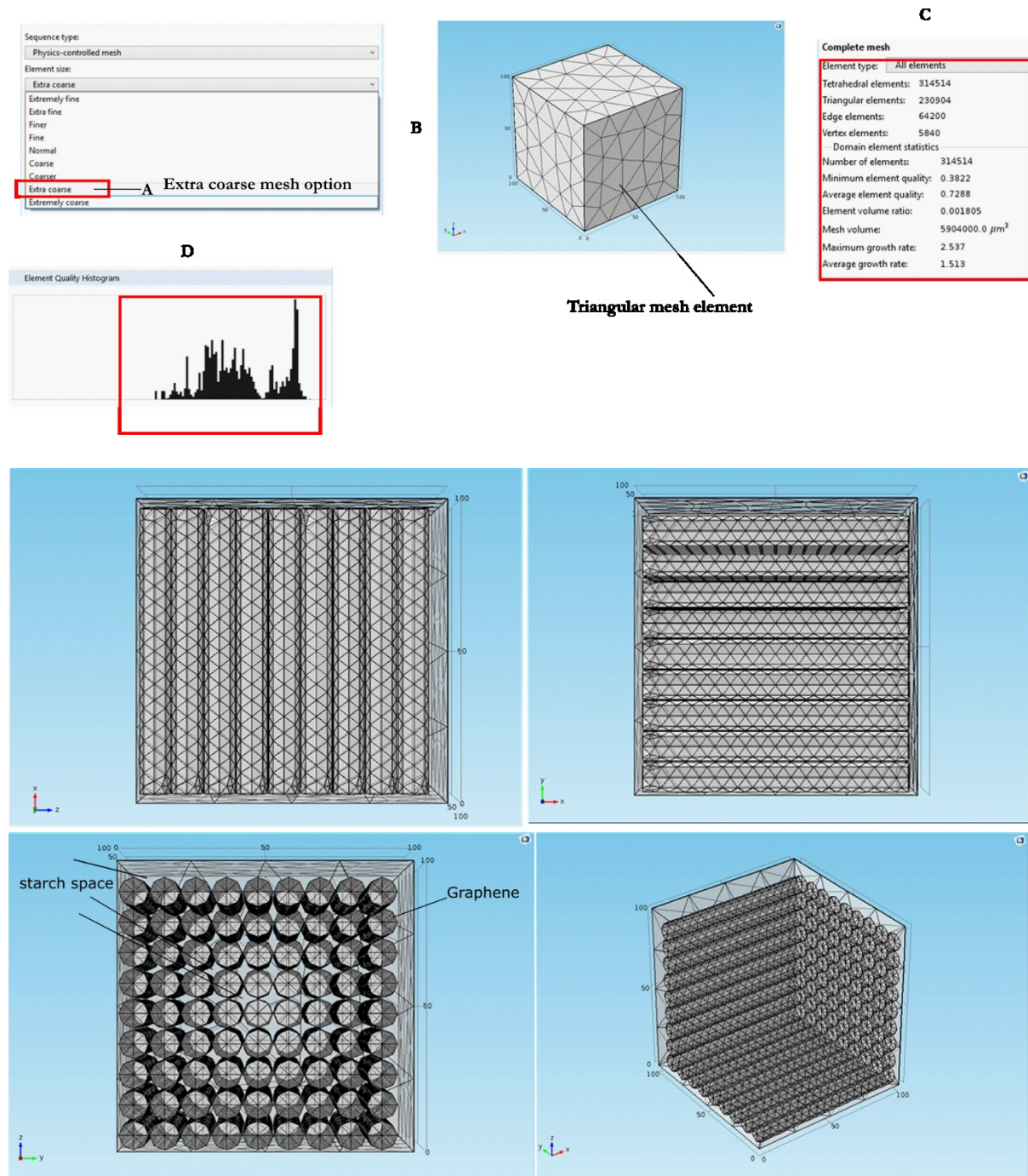
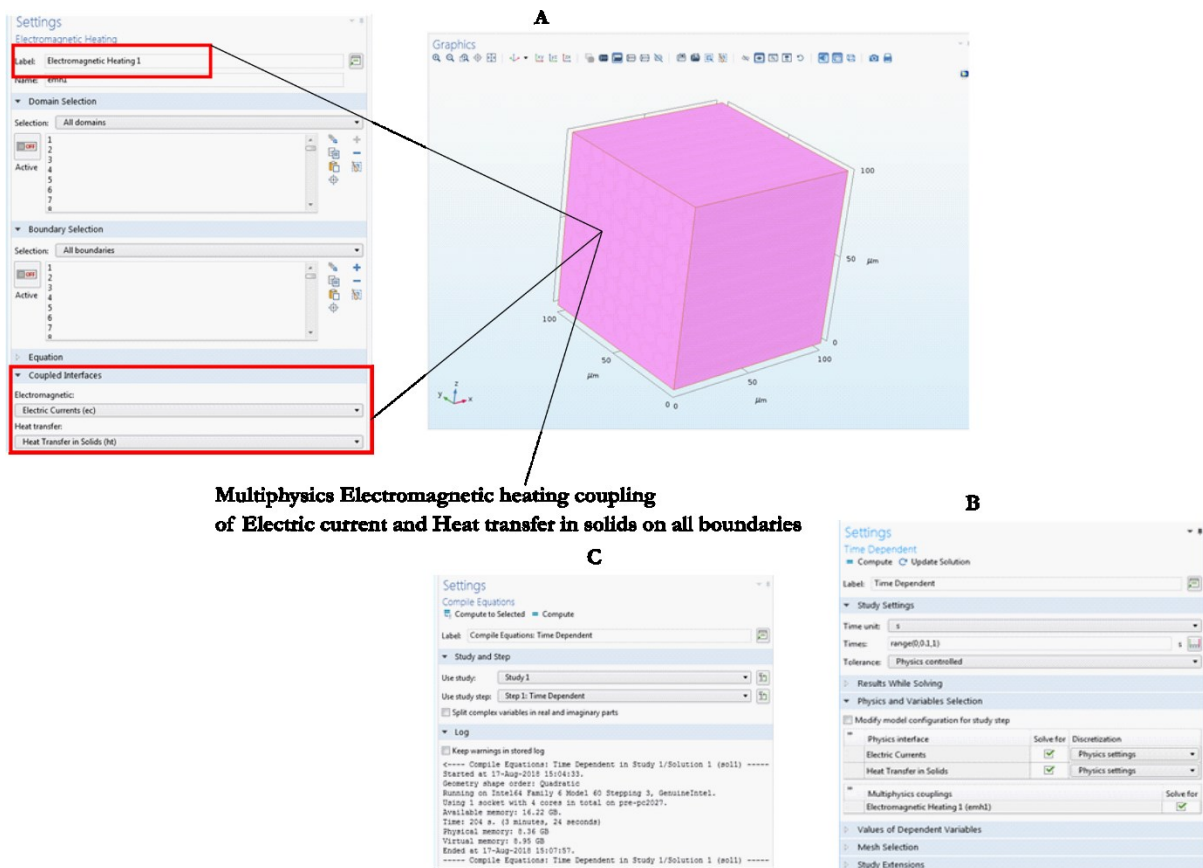


Figure 12 Mesh details A; mesh controlled physics sequence type B; Triangular mesh elements C; Complete mesh statistics D; Mesh histogram; xz, zy, yx and the xyz planes

The Multiphysics coupling in COMSOL is a two-way coupling of the electric current and the heat transfer in solids. The electromagnetic heating is used to combine the two physical domains as shown in the Fig.13. The 3 lines in A clearly illustrate the connection between the physics and all the boundaries of the graphene-starch composite.

The time dependent solver settings are shown in Fig.13 B, which provides the tools for selecting the units of time, the range of the solver and the tolerance. It also provides the option of solving one physics and using the results of the preceding solved physics as initial values to the solving the second physics. In this simulation, the electric current and the heat transfer in solids were solved simultaneously. A simultaneous solution is enabled using the two solve for discretisation check box as shown in Fig. 13 B.

The compiled equation window screen shot in Fig. 13 C, populate the multi-line textbox with the solver compilations with geometric shape order and the computer hardware configurations and the time it takes for the solution to converge, in this case the solution converged after 204 s. The graphic details are expanded in Fig. 14. The time dependent and the segregated solver convergence plots (Fig.4) shows the transition solution time step, reciprocal of the step size, error and iteration number as the solver compute the solution to the electric current equations (Maxwell) and the heat transfer in solids equations (Fourier) over the composite domain.



Multiphysics Electromagnetic heating coupling of Electric current and Heat transfer in solids on all boundaries

Fig. 13 (A) Electromagnetic heating coupling of electric and heat transfer in solids settings; (B) time dependent solver and settings; (C) Compiled equations log settings

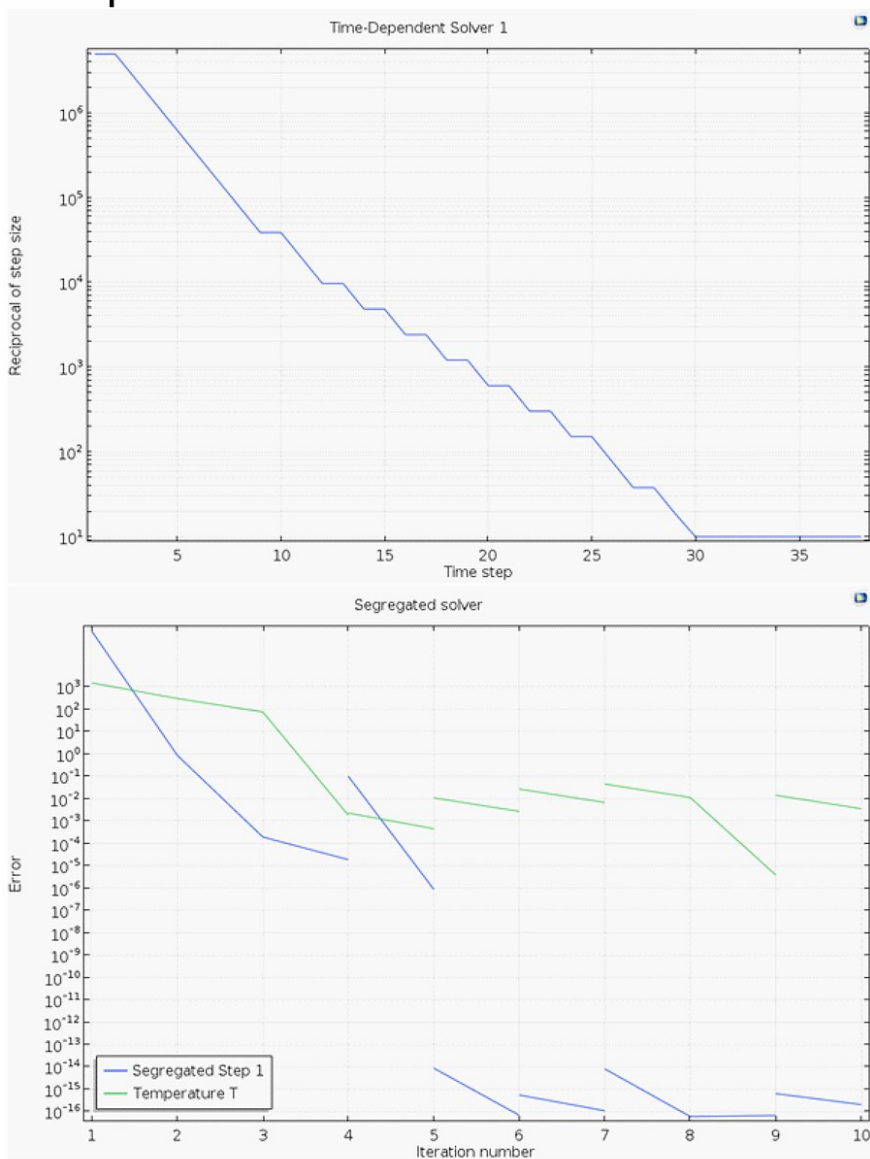
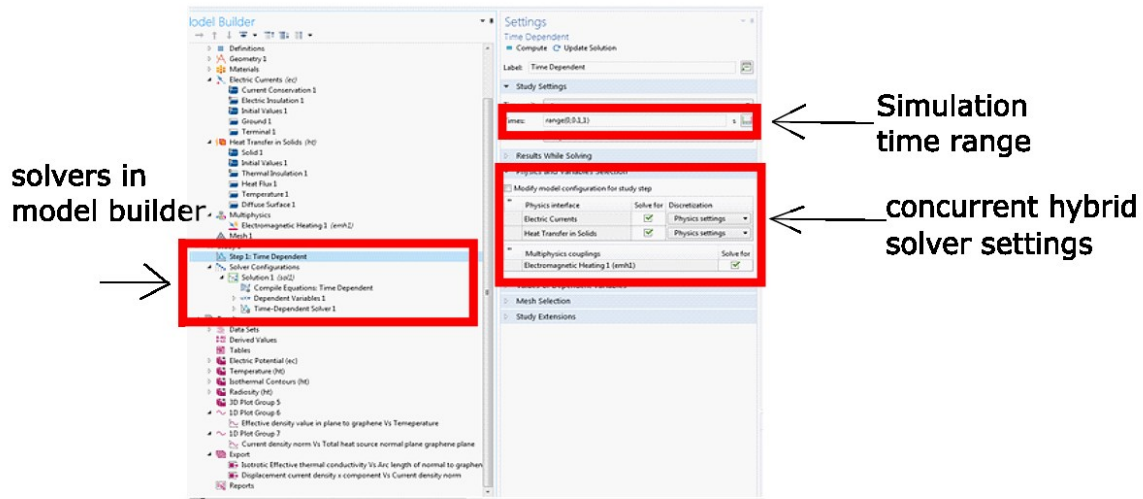


Fig. 14 Time dependent and segregated solver convergence plot

The segregated solver functions are to combine the dependent variables (temperature, electric current, electric potential and velocity) and use the values of the dependent variables to solve for the effective properties of the composite. The procedures are repeated several times until the solution converges. This is shown on the time dependent solver convergence plot at precisely 30 time step.

4.2 Results and post-processing

The results obtained were post-processed using the tools provided in the COMSOL model builder window. The simulation is in 3d as result a 3d cut line, normal and in-plane to the to the graphene fibre array was created to enable x-y plotting of the plot groups. The 3d cut line plots implementation is shown in “3d cut line” normal and in-plane to the graphene fibre array in Fig.15.

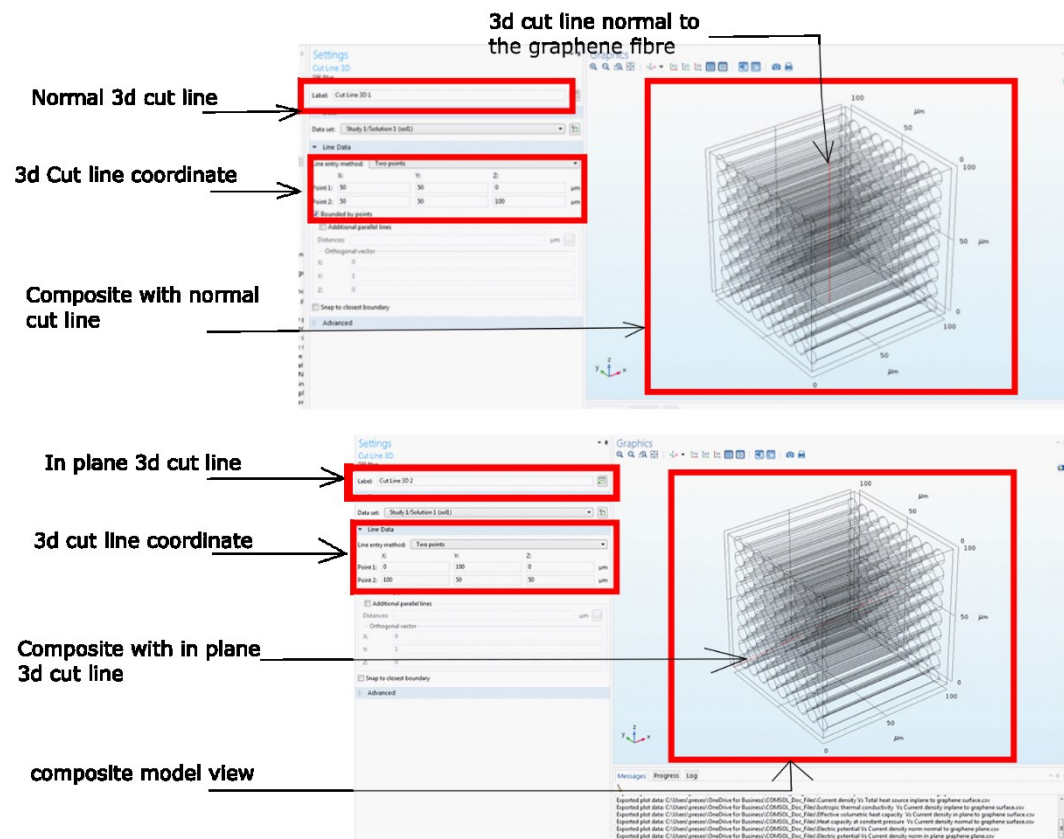


Fig. 15 3d cut line normal and in-plane to the graphene fibre array

The visualisation of the electric field especially as the electromagnetic heating propagate through the composite, from the terminal to the ground face provides and understanding of it effect on the material properties. It also gives a bird-eye view of the electric field driven non-stationary heat transport. The possibilities of the state of the art are limitless. A full-scale animation of the Multiphysics transitions can be implemented with the animation tool in the model builder window.

The multislice electric potential colour plot shows the direction of travel from the terminal with red and orange colour to blue colour at the ground face as shown in the electric potential Multislice plot of the graphene-starch composite in Fig. 16.

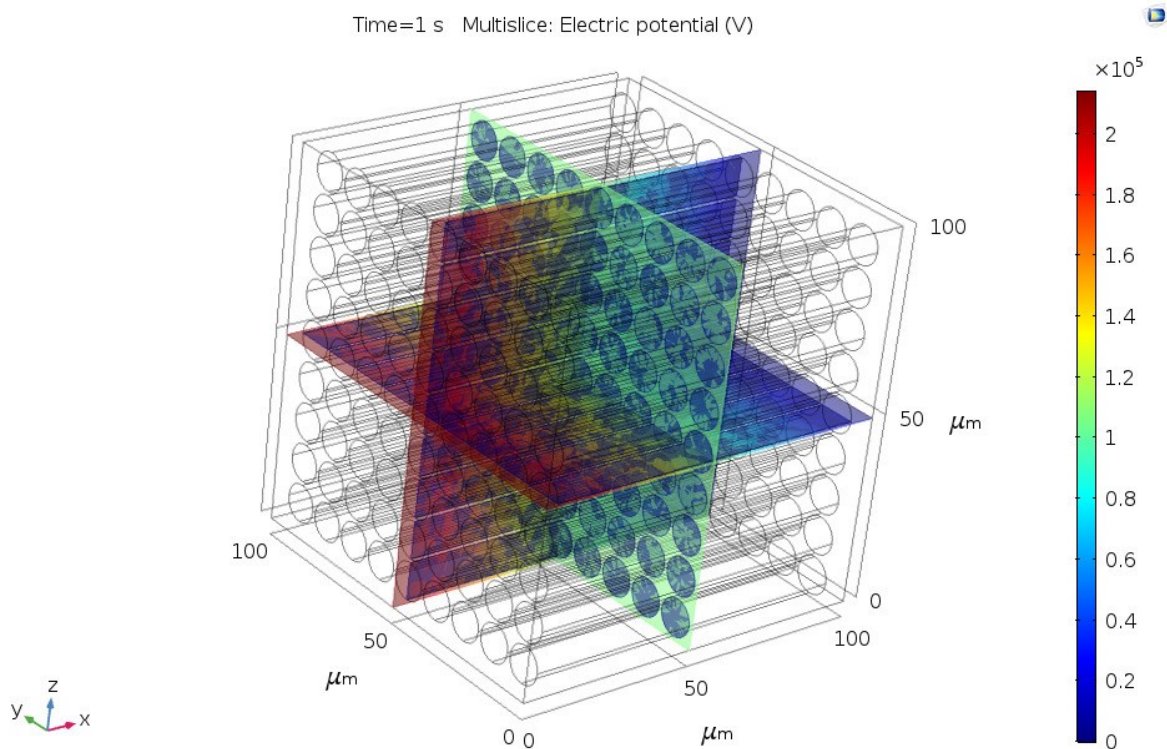


Fig. 16 Electric potential Multislice plot of the graphene-starch composite

The Multislice plot is used to display or show the potential difference as a scalar quantity on slices in xz , yz and xy planes intersecting at right angles. It provides the increase in the potential differences from the ground face to the electric terminal face. The values display on the colour bar is to be multiply by a factor of 10^{-6} , because of the dimension scale of the composite (μm)

The surface and isosurface colour plot as shown in Surface and Isosurface temperature colour map plot of the graphene-starch composite in Fig. 17, is a visualisation of the temperature time evolution through the boundaries and entire domain of the graphene-starch composite. The bottom face and the top phases of the composite are at lower temperatures marked by the red colour. The temperature evolves from the top and the bottom towards the centre of the composite

The Isosurface temperature shows the temperature as a set of coloured surfaces with constant temperature values. It is used to visualised the temperature as a scalar field.

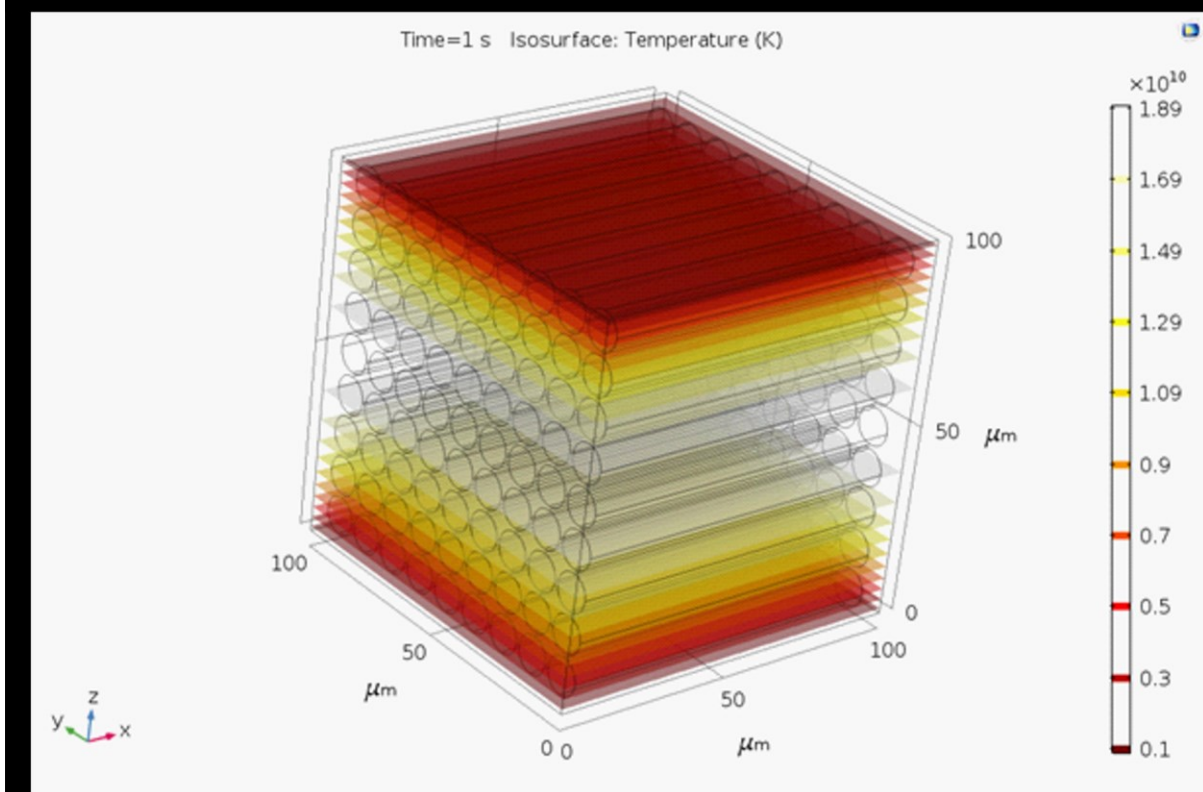
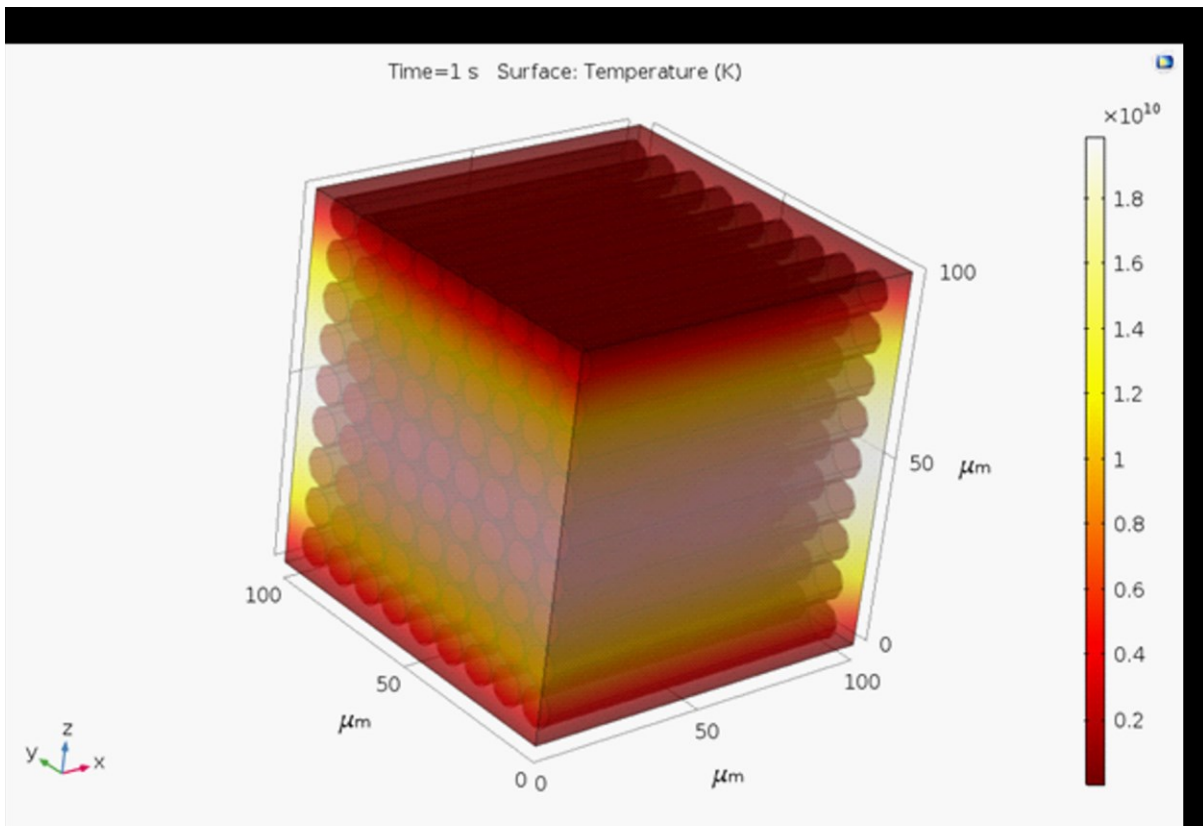


Fig.17 Surface and Isosurface temperature colour map plot of the graphene-starch composite

The normal current density in Fig. 18 is a surface contour of the current flow vector from the high current at the terminal boundary where the 15 A is applied to the ground face where a zero potential is applied. The direction of flow is indicated by the red arrows.

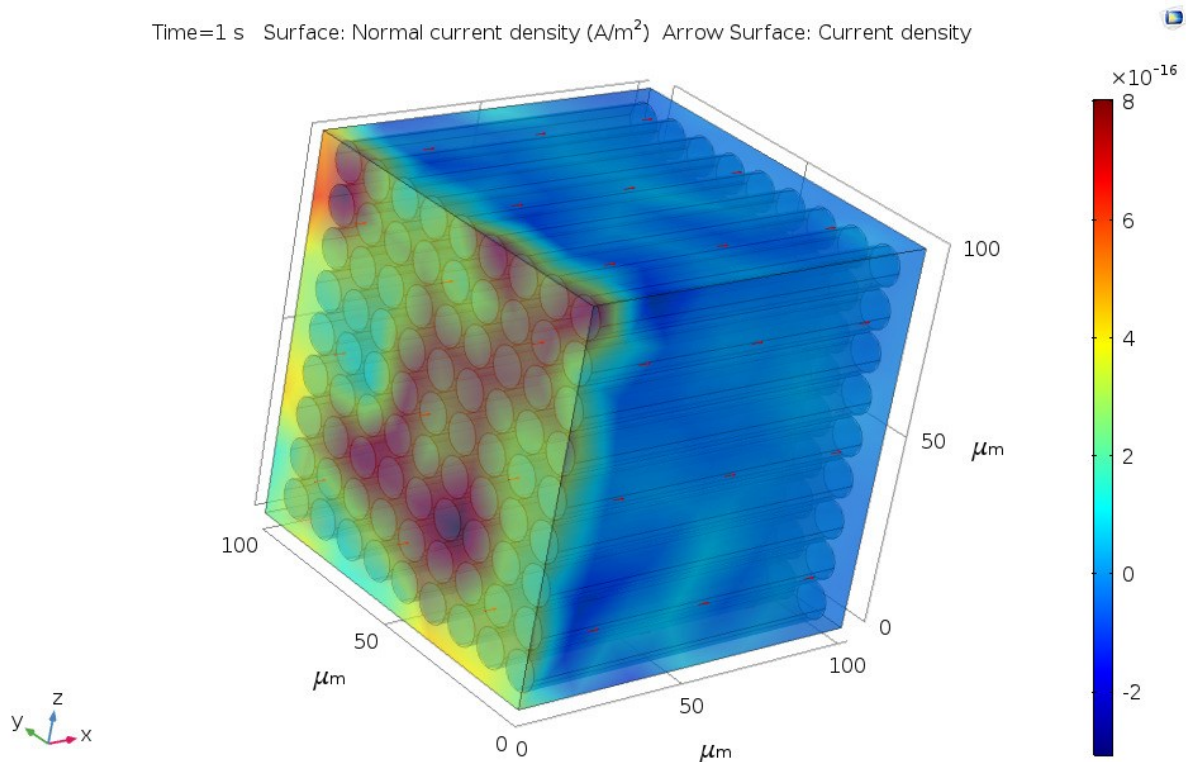


Fig.18 Surface normal current density and arrow surface plot of the graphene-starch composite

The displacement current in the Maxwell equation increases with the current density as shown in Fig. 19 A. It also shows that the displacement current and the current density remain constant during the simulation. The potential difference and the current density; the current density and the total heat source shows a similar trend as shown in Figs. 19 B and C. The effective thermal conductivity decreases with an increase in temperature. The physical properties (effective thermal conductivity), changes with time as seen in the different plot lines at different simulation time. The trend is expected the current density changes from the electrical terminal to the ground face of the composite. The converse is true for the specific heat capacity and the effective density of the composite. The specific heat capacity at constant pressure and the effective densities increase with temperature in plane and normal to the plan of the graphene fibres. These trends, reveal that the properties are dependent on the orientation of the fibre in a composite as shown in Fig. 20.

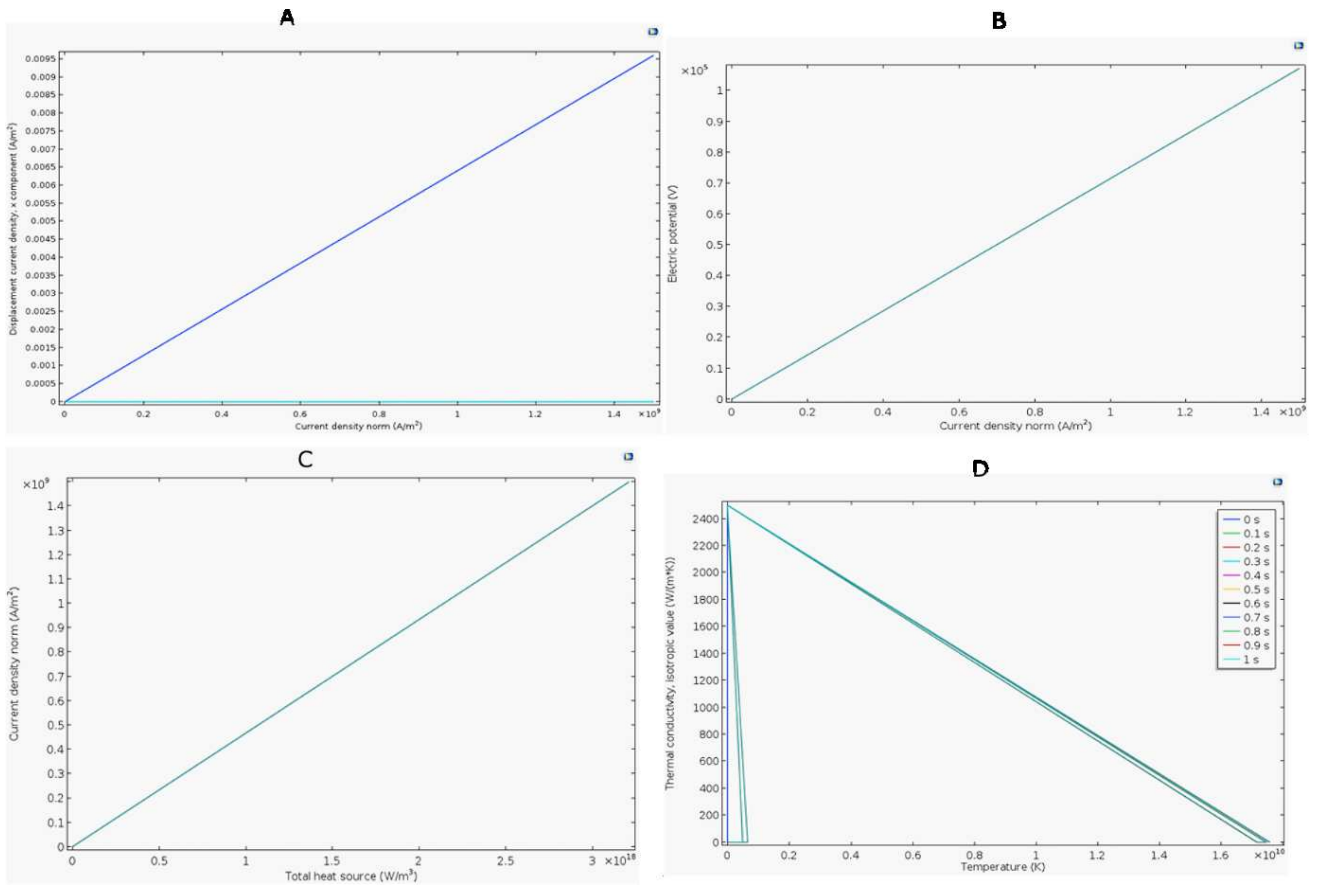


Fig. 19 Displacement current, Electric potential, current density, total heat source, Isotropic Effective thermal conductivity

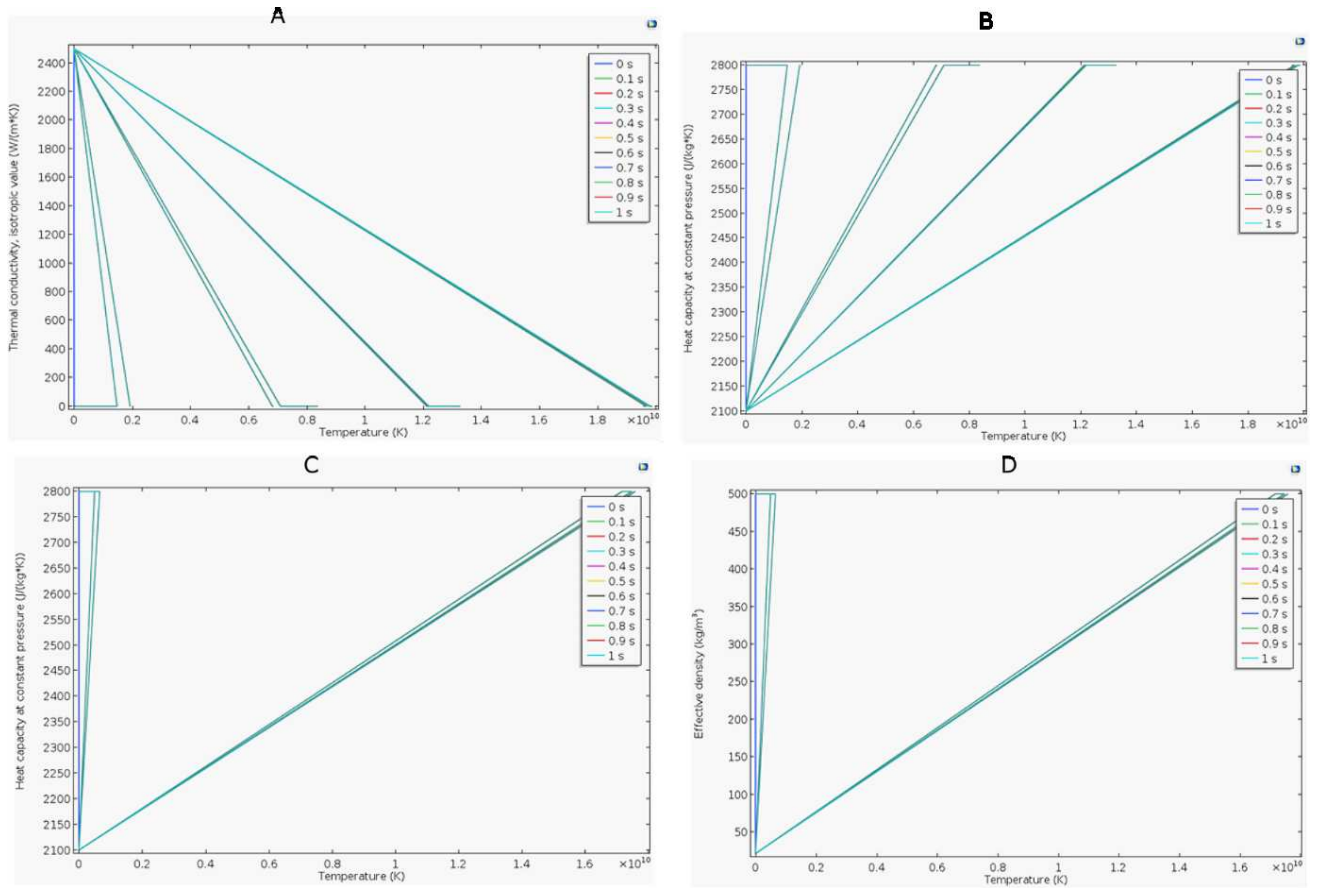


Fig. 20 Effective isotropic thermal conductivity, Effective heat capacities at constant pressure and Effective density of the composite as function of temperature

5 Conclusions and future research scope

In this chapter, we have described a COMSOL Multiphysics Finite Element modelling and simulation of a graphene-starch composite in 3-dimensional space. The graphics driven with windows screen shots are included to serve as guide to interested readers who wish to model the conductivity of a composite following our approach. The model can be refined and the simulation time can be extended with refined meshing to increase the accuracy of the physical properties predicted by COMSOL Multiphysics software package.

It was observed here that the electrical properties are isotropic and the properties remain the same irrespective of the direction of the orientation (in-plane or normal) of the graphene cylindrical fibres. On the other hand, the thermal properties seem to exhibit and anisotropic behaviour and changes with time and the orientation with respect to the graphene fibre. A detailed analysis of the composite with all the rigour of different orientation of the graphene fibres as different studies is beyond the scope of the current chapter but could be studied in future.

Furthermore, a more rigorous treatment of the anisotropic thermal property dependencies of the cylindrical graphene composite could be investigated in future. The Multiphysics tool is capable of handling more physics such as structural mechanics effect as consequence of electromagnetic heating to how this effect the stress, strain and yield of the resulting composite. The effect of prolong heating to the creep behavioural changes to the composite can also be investigated using the Multiphysics tool in future.

6 References

- [1] Zalba B, Marin JM, Cabeza LFLF, Mehling H, Marín JM, Cabeza LFLF, et al. Review on thermal energy storage with phase change: materials, heat transfer analysis and applications. 2003. doi:10.1016/S1359-4311(02)00192-8.
- [2] Tsai SW. Theory of Composites Design. Theory Compos by Graeme W Milton, Pp 748 ISBN 0521781256 Cambridge, UK Cambridge Univ Press May 2002 2008.
- [3] Gong F, Duong H, Papavassiliou D. Review of Recent Developments on Using an Off-Lattice Monte Carlo Approach to Predict the Effective Thermal Conductivity of Composite Systems with Complex Structures. Nanomaterials 2016. doi:10.3390/nano6080142.
- [4] Liu Q, He XB, Ren S Bin, Liu TT, Kang QP, Qu XH. Fabrication and thermal conductivity of copper matrix composites reinforced with Mo₂C or TiC coated graphite fibers. Mater Res Bull 2013. doi:10.1016/j.materresbull.2013.07.064.
- [5] Eian CS, Deissler RG. Effective thermal conductivities of magnesium oxide, stainless steel, and uranium oxide powders in various gases. Library (Lond) 1953.
- [6] Wakao N, Kato K. Effective Thermal Conductivity of Packed Beds. J Chem Eng JAPAN 1969. doi:10.1252/jcej.2.24.
- [7] Tsotsas E, Martin H. Thermal conductivity of packed beds: A review. Chem Eng Process 1987. doi:10.1016/0255-2701(87)80025-9.
- [8] Cheng G. Evaluation of effective thermal conductivity from the structure of a packed bed. Chem Eng Sci 1999. doi:10.1016/S0009-2509(99)00125-6.
- [9] The Automotive Research Association of India. Air Quality Monitoring and Emission Source Apportionment Study for Pune. 2010. doi:December 2010.
- [10] Furmanski P. Effective macroscopic description for heat conduction in heterogeneous materials. Int J Heat Mass Transf 1992. doi:10.1016/0017-9310(92)90324-L.
- [11] Ishai O, Cohen LJ. Elastic properties of filled and porous epoxy composites. Int J Mech Sci 1967. doi:10.1016/0020-7403(67)90053-7.
- [12] Muric-Nesic J, Compston P, Stachurski ZH. On the void reduction mechanisms in vibration assisted consolidation of fibre reinforced polymer composites. Compos Part A Appl Sci Manuf 2011. doi:10.1016/j.compositesa.2010.12.011.
- [13] Chen H, Xu Q, Chen S, Zhang Z. Evaluation and design of fiber-reinforced asphalt mixtures. Mater Des 2009. doi:10.1016/j.matdes.2008.09.030.

- [14] GHIORSE SR. Effect of void content on the mechanical properties of carbon/epoxy laminates. SAMPE Q 1993. doi:10.1034/j.1600-0447.2001.00166.x.
- [15] Kamiuto K, Yee SS. Heat transfer correlations for open-cellular porous materials. Int Commun Heat Mass Transf 2005. doi:10.1016/j.icheatmasstransfer.2004.10.027.
- [16] Kamiuto K. Modeling of Composite Heat Transfer in Open-Cellular Porous Materials at High Temperatures. Cell. Porous Mater. Therm. Prop. Simul. Predict., 2008. doi:10.1002/9783527621408.ch6.
- [17] Matt CF, Cruz ME. Calculation of the effective conductivity of ordered short-fiber composites. 35th AIAA Thermophys. Conf., 2001. doi:doi:10.2514/6.2001-2968.
- [18] Anis-ur-Rehman M, Maqsood A. A modified transient method for an easy and fast determination of thermal conductivities of conductors and insulators. J Phys D Appl Phys 2002. doi:10.1088/0022-3727/35/16/320.
- [19] Ahadi M, Andisheh-Tadbir M, Tam M, Bahrami M. An improved transient plane source method for measuring thermal conductivity of thin films: Deconvoluting thermal contact resistance. Int J Heat Mass Transf 2016. doi:10.1016/j.ijheatmasstransfer.2016.01.037.
- [20] Kuvandykova D, St-Laurent R. Application of the Modified Transient Plane Source Technique in Testing the Thermal Conductivity of Concrete. Proc. 31st Int. Therm. Conduct. Conf. 19th Int. Therm. Expans. Symp., 2010.
- [21] Boutinguiza M, Lusquiños F, Pou J, Soto R, Quintero F, Comesaña R. Thermal properties measurement of slate using laser flash method. Opt Lasers Eng 2012. doi:10.1016/j.optlaseng.2011.11.016.
- [22] Tada Y, Harada M, Tanlgaki M, Eguchi W. Laser Flash Method for Measuring Thermal Conductivity of Liquids. Application to Molten Salts. Ind Eng Chem Fundam 1981. doi:10.1021/i100004a005.
- [23] Dos Santos WN, Mummery P, Wallwork A. Thermal diffusivity of polymers by the laser flash technique. Polym Test 2005. doi:10.1016/j.polymertesting.2005.03.007.
- [24] Min S, Blumm J, Lindemann A. A new laser flash system for measurement of the thermophysical properties. Thermochim Acta 2007. doi:10.1016/j.tca.2006.11.026.
- [25] COMSOL Multiphysics. Introduction to COMSOL Multiphysics 5.0. Manual 2009.
- [26] Comsol. MODELING GUIDE Multiphysics COMSOL. 2010. doi:10.1007/s10237-010-0257-z.
- [27] Comsol. Heat Transfer Module: User's Guide. Heat Transf Modul User's Guid 2012. doi:http://www.evp.rpi.edu/hartford/~collir5/MP/OTHER/Reference/HeatTransferModuleUsersGuide.pdf.
- [28] COMSOL. COMSOL Multiphysics® Modeling Software. COMSOL 2016. doi:10.1007/s11356-015-5536-x.
- [29] Wang BX, Zhou LP, Peng XF. A fractal model for predicting the effective thermal conductivity of liquid with suspension of nanoparticles. Int J Heat Mass Transf 2003. doi:10.1016/S0017-9310(03)00016-4.
- [30] Zhao CY, Lu TJ, Hodson HP, Jackson JD. The temperature dependence of effective thermal conductivity of open-celled steel alloy foams. Mater Sci Eng A 2004. doi:10.1016/j.msea.2003.10.241.

- [31] Mangal R, Saxena NS, Sreekala MS, Thomas S, Singh K. Thermal properties of pineapple leaf fiber reinforced composites. *Mater Sci Eng A* 2003. doi:10.1016/S0921-5093(02)00166-1.
- [32] Gonzo EE. Estimating correlations for the effective thermal conductivity of granular materials. *Chem Eng J* 2002. doi:10.1016/S1385-8947(02)00121-3.
- [33] Nicholls JR, Lawson KJ, Johnstone A, Rickerby DS. Methods to reduce the thermal conductivity of EB-PVD TBCs. *Surf Coatings Technol* 2002. doi:10.1016/S0257-8972(01)01651-6.
- [34] Kumlutaş D, Tavman IH, Turhan Çoban M. Thermal conductivity of particle filled polyethylene composite materials. *Compos Sci Technol* 2003. doi:10.1016/S0266-3538(02)00194-X.
- [35] Elsari M, Hughes R. Axial effective thermal conductivities of packed beds. *Appl Therm Eng* 2002. doi:10.1016/S1359-4311(02)00117-5.
- [36] Asako Y, Kamikoga H, Nishimura H, Yamaguchi Y. Effective thermal conductivity of compressed woods. *Int J Heat Mass Transf* 2002. doi:10.1016/S0017-9310(01)00330-1.
- [37] Milton GW. *The Theory of Composites* 2002. doi:10.1017/CBO9780511613357.
- [38] Furmanski P. Influence of Different Parameters on the Effective Thermal Conductivity of Short-Fiber Composites. *J Thermoplast Compos Mater* 1991. doi:10.1177/089270579100400403.
- [39] Mirmira SR, Fletcher LS. Review of the thermal conductivity of thin films. *J Thermophys Heat Transf* 1998. doi:10.2514/2.6321.
- [40] Zhang YF, Zhao YH, Bai SL, Yuan X. Numerical simulation of thermal conductivity of graphene filled polymer composites. *Compos Part B Eng* 2016. doi:10.1016/j.compositesb.2016.09.052.
- [41] Tekce HS, Kumlutas D, Tavman IH. Effect of particle shape on thermal conductivity of copper reinforced polymer composites. *J Reinf Plast Compos* 2007. doi:10.1177/0731684407072522.
- [42] Shonnard DR, Whitaker S. The effective thermal conductivity for a pointcontact porous medium: an experimental study. *Int J Heat Mass Transf* 1989. doi:10.1016/0017-9310(89)90138-5.
- [43] Auriault JL, Ene HI. Macroscopic modelling of heat transfer in composites with interfacial thermal barrier. *Int J Heat Mass Transf* 1994. doi:10.1016/0017-9310(94)90342-5.
- [44] Auriault JL. Wave propagation and transient heat transfer in thermoelastic composites. *Int J Heat Mass Transf* 2012. doi:10.1016/j.ijheatmasstransfer.2012.06.007.
- [45] Ramani K, Vaidyanathan A. Finite Element Analysis of Effective Thermal Conductivity of Filled Polymeric Composites. *J Compos Mater* 1995. doi:10.1177/002199839502901304.
- [46] Liang JZ. Heat transfer in polymer composites filled with inorganic hollow micro-spheres. *Adv Struct Mater* 2011. doi:10.1007/8611_2010_3.
- [47] Fiedler T, Löffler R, Bernthaler T, Winkler R, Belova I V., Murch GE, et al. Numerical analyses of the thermal conductivity of random hollow sphere structures. *Mater Lett* 2009. doi:10.1016/j.matlet.2008.10.030.

- [48] Fiedler T, Richards HS, Belova I V., Öchsner A, Murch GE. Experimental analysis on the thermal anisotropy of syntactic hollow sphere structures. *Exp Therm Fluid Sci* 2013. doi:10.1016/j.expthermflusci.2012.09.003.
- [49] Fiedler T, Belova I V., Öchsner A, Murch GE. Non-linear calculations of transient thermal conduction in composite materials. *Comput Mater Sci* 2009. doi:10.1016/j.commatsci.2008.10.021.
- [50] Vian A, Davies E, Gendraud M, Bonnet P. Plant Responses to High Frequency Electromagnetic Fields. *Biomed Res Int* 2016. doi:10.1155/2016/1830262.
- [51] Bridges JE, Krstansky JJ, Taflove A, Sresty GC. IITRI IN SITU RF FUEL RECOVERY PROCESS. *J Microw Power* 1983. doi:10.1080/16070658.1983.11689305.
- [52] Alboudwarej H, Felix J, Taylor S, Badry R, Bremner C, Brough B, et al. Highlighting heavy oil. 2006.
- [53] Hashemi R, Nassar NN, Pereira Almaso P. Nanoparticle technology for heavy oil in-situ upgrading and recovery enhancement: Opportunities and challenges. *Appl Energy* 2014. doi:10.1016/j.apenergy.2014.07.069.
- [54] Nasr TN, Ayodele OR. Thermal Techniques for the Recovery of Heavy Oil and Bitumen. *SPE Int. Improv. Oil Recover. Conf. Asia Pacific*, 2005. doi:10.2118/97488-MS.
- [55] Shah A, Fishwick R, Wood J, Leeke G, Rigby S, Greaves M. A review of novel techniques for heavy oil and bitumen extraction and upgrading. *Energy Environ Sci* 2010. doi:10.1039/b918960b.
- [56] Davison RJ. Electromagnetic Stimulation of Lloydminster Heavy Oil Reservoirs: Field Test Results. *J Can Pet Technol* 1995. doi:10.2118/95-04-01.
- [57] Sayegh SG, Maini BB. Laboratory Evaluation of the CO₂ Huff-N-Puff Process for Heavy Oil Reservoirs. *J Can Pet Technol* 1984. doi:10.2118/84-03-02.
- [58] Sayegh SG, Maini BB. Laboratory Evaluation Of The CO₂ Huff-N-Puff Process For Heavy Oil Reservoirs. *J Can Pet Technol* 1984. doi:10.2118/84-03-02.
- [59] Keyes DE, McInnes LC, Woodward C, Gropp W, Myra E, Pernice M, et al. Multiphysics simulations: Challenges and opportunities. *Int J High Perform Comput Appl* 2013. doi:10.1177/1094342012468181.
- [60] Gallardo LA, Meju MA. Structure-coupled multiphysics imaging in geophysical sciences. *Rev Geophys* 2011. doi:10.1029/2010RG000330.
- [61] Gaston DR, Permann CJ, Peterson JW, Slaughter AE, Andrš D, Wang Y, et al. Physics-based multiscale coupling for full core nuclear reactor simulation. *Ann Nucl Energy* 2015. doi:10.1016/j.anucene.2014.09.060.